HHS Public Access

Author manuscript

Acta Biomater. Author manuscript; available in PMC 2019 November 13.

Published in final edited form as:

Acta Biomater. 2019 November ; 99: 1–17. doi:10.1016/j.actbio.2019.08.017.

Biomechanics of aortic wall failure with a focus on dissection and aneurysm: A review

Selda Sherifova[a], **Gerhard A. Holzapfel**[a,b,*]

[a]Institute of Biomechanics, Graz University of Technology, Stremayrgasse 16/2, 8010 Graz, Austria

[b]Department of Structural Engineering, Norwegian Institute of Science and Technology (NTNU), 7491 Trondheim, Norway

Abstract

Aortic dissections and aortic aneurysms are fatal events characterized by structural changes to the aortic wall. The maximum diameter criterion, typically used for aneurysm rupture risk estimations, has been challenged by more sophisticated biomechanically motivated models in the past. Although these models are very helpful for the clinicians in decision-making, they do not attempt to capture material failure. Following a short overview of the microstructure of the aorta, we analyze the failure mechanisms involved in the dissection and rupture by considering also traumatic rupture. We continue with a literature review of experimental studies relevant to quantify tissue strength. More specifically, we summarize more extensively uniaxial tensile, bulge inflation and peeling tests, and we also specify trouser, direct tension and in-plane shear tests. Finally we analyze biomechanically motivated models to predict rupture risk. Based on the findings of the reviewed studies and the rather large variations in tissue strength, we propose that an appropriate material failure criterion for aortic tissues should also reflect the microstructure in order to be effective.

Keywords

Aortic dissection; Aortic aneurysm; Aortic failure; Aortic microstructure; Tissue strength; Uniaxial tensile test; Bulge inflation test; Peeling test; Rupture risk

1. Introduction

Aortic dissection and aortic aneurysm rupture are acute life threatening events. Overall mortality rates of dissections and aneurysms of the thoracic aorta remain high despite the improvements over the years [93,138,97]. Ruptured aneurysms of the abdominal aorta are estimated to cause 4–5% of sudden deaths in the United States, and the event of rupture has mortality rates as high as 80% [119].

*Corresponding author at: Institute of Biomechanics, Graz University of Technology, Stremayrgasse 16/2, 8010 Graz, Austria. holzapfel@tugraz.at (G.A. Holzapfel).

Aortic dissection is an acute condition of the aorta which typically starts with an intimal tear to the presumably already weakened wall, followed by a crack in the radial direction. The crack then proceeds within the medial layer, or between the media and the adventitia, causing the layers of the aortic wall to separate, thereby creating a false lumen where the blood can flow into [83,58]. This leads to a dilatation and a further weakening of the intact outer wall of the false lumen. In most fatal conditions, the aorta bursts causing the patient to bleed to death quickly [91,24]. Stanford type A dissections - affecting the ascending aorta - are shown to become chronic only rarely, whereas type B dissections - affecting the descending thoracic aorta only - are routinely chronic with a thickened, straightened intimal flap which lost its mobility due to remodeling [101]. Approximately 67% of the cases are reported to be type A dissections [97]. The risk factors include but are not limited to age, hypertension, smoking, congenital disorders such as bicuspid aortic valve (BAV), genetic disorders such as Marfan syndrome and Ehlers-Danlos syndrome [57,33]. Intimal tears leading to ascending aortic dissection are typically located a few centimeters above the coronary arteries, whereas the ones leading to descending aortic dissection are located a few centimeters beyond the left subclavian artery [33]. For a mechanical assessment of arterial dissections see the review article by Tong et al. [142]. Fig. 1(a) illustrates the basic anatomy of the aorta, while the sketch in Fig. 1(b) shows a dissected wall with arrows indicating the blood flow.

Aortic aneurysms are local dilatations of the aorta, typically more than 50% of the normal diameter [41]. The underlying mechanisms leading to aneurysm formation differ between the ascending aorta and the descending thoracic aorta [117], as well as between the thoracic and the abdominal aorta [33,116,14] due to different embryonic origins of the cells involved in the remodeling process. The aneurysms in the ascending aorta are usually not accompanied by atherosclerosis, whereas in the descending thoracic and the abdominal aorta it is a common finding [57]. Nevertheless, all aneurysms are characterized by alterations to the extracellular matrix. For a review on the biomechanics, mechanobiology, and modeling of aneurysms see Humphrey & Holzapfel [54].

In addition to the above mentioned pathologies, thoracic aortic trauma is accountable for a large percentage of losses involving motor vehicle accidents, and it can initiate the dissection process or cause an immediate rupture. Bertrand et al. [4] reported 1.2% of the occupants involved in vehicular accidents sustained a traumatic injury of the aorta, of which 94% were deadly, accounting for 21.4% of all fatalities. Traumatic aortic injury can also be due to heavy falls on feet, airplane crashes, suicide attempts, or surgical procedures [51,121,46]. The ascending aorta is reported to be the most common injury site due to trauma [78], whereas the aortic isthmus has been identified as the most vulnerable location for injury by several studies [23,126,4] constituting a number as high as 90% [23], followed by the aortic arch and the abdominal aorta around the bifurcations.

To prevent further complications such as rupture, dilatations of the aorta due to aneurysm or aortic dissection are surgically treated if the maximum diameter of the lesion is above 5.0 cm in women or 5.5 cm in men, or if the maximal diameter increases more than 0.51 cm in one year [69,45,43]. Clinicians consider several indicators before decision-making about a surgical intervention - such indicators include maximum diameter, expansion rate, genetic

risk factors and the family history just to name a few. For example, the maximum diameter criterion is revised if the patient suffers from a connective tissue disorder such as Marfan syndrome, see Brownstein et al. [9], and Fig. 1 therein. Even though it has been shown that the risk of rupture and dissection of aneurysms increase significantly at sizes larger than 6 cm for the thoracic aorta [26], this criterion is in contradiction with the observation that aneurysms can rupture or dissect at any diameter [11,98,154,97,117], and it ignores the more complex relationships between the rupture and the material properties such as the heterogeneity of tensile strength in the wall of aortic aneurysms [149]. Clinicians need more reliable tools to assess the risk of intervention versus the risk of rupture, as the maximum diameter criterion can underestimate the rupture risk of smaller aneurysms, and overestimate it for the larger ones.

To gain a more in-depth understanding of the possible mechanisms leading to these fatal events, this review analyzes experimental studies that aim to quantify the strength of aortic walls towards a material failure perspective and reviews biomechanically motivated models to predict rupture risk. After summarizing the microstructure of the aorta in Section 2, we continue with a brief account of damage and failure mechanisms involved in the dissection and rupture in Section 3. Subsequently, in Section 4 we summarize some important experimental studies that quantify the strength, and in Section 5 we summarize the state-of-the-art on the biomechanics-based rupture risk prediction models for clinical use. Finally, within Section 6, we provide concluding remarks. Readers interested in damage models or computational aspects of failure are referred to, e.g., the two recent book chapters of Holzapfel & Fereidoonnezhad [52] and Gultekin & Holzapfel [44], respectively.

2. Microstructure

We continue with a glance at the structure of the aorta as it provides a basis for our discussion. The aorta is composed of the intima, media and adventitia, as shown in Fig. 2(a). The intima is mechanically negligible in a young and healthy aorta, and it is basically a single layer of endothelial cells [53]. This layer becomes mechanically significant, especially with age, due to non-atherosclerotic intimal thickening during which collagen fibers are deposited [12]. Fig. 2(a) shows a sketch of such an artery with intimal thickening, while Fig. 2(b) partly depicts the collagen architecture of a healthy (but aged) wall obtained from an abdominal aorta and produced with second-harmonic generation microscopy. The media consists of several concentric lamellar units bound together, see Fig. 2(a) and (c). Each of these units contains smooth muscle cells with their radially tilted longer axes oriented at an angle closer to the circumferential direction, surrounded by collagen fibers embedded in the extracellular matrix [94], see Fig. 2(c), (d). Collagen in the media is typically present as two symmetric families of fibers with a mean orientation closer to the circumferential direction, whereas in the adventitia the mean orientation is closer to the longitudinal direction [120]. The media is the main load bearing layer for physiological loads, and the adventitia acts as a stiff jacket-like tube at higher levels of pressure, which prevents the artery from overstretch and rupture [53]. The thickness of the thoracic aortic media go hand in hand with an increase in the number of lamellar units, and the thickness of a single lamellar unit is constant amongst mammalian species (approximately 15 im) [165,166]. However, human abdominal aortas have fewer lamellae for a given thickness

compared to other species [166]. Growth of the human thoracic aorta is thought to be primarily due to the increase in the number of lamellar units, whereas in the human abdominal aorta it is mainly due to the increase in the thickness of the lamellar units [164].

A key structural change in thoracic aortic dissections is the so-called medial degeneration, as first reported by Erdheim [34]. Typically, it involves smooth muscle cell loss, elastic fiber fragmentation, and an accumulation of proteoglycans [8,5,167]. A weakened aortic wall due to medial degeneration is also typical for aneurysms and dissecting aneurysms of the ascending aorta [6], not only with tricuspid aortic valve (TAV) but also with BAV and bovine aortic arch phenotypes [102], see Fig. 3(a)–(f) for examples of proteoglycan accumulation zones. Versican and aggreacan were identified as the major components of such accumulations in thoracic aortic aneurysm and dissection patients [20]. In addition, one can see a change in the elastic fiber structure of a dissected aorta (Fig. 3(g)) where the elastic structure connecting the lamellar units are highly degenerated compared to a control aorta (Fig. 3(h)) [87]. Collagen content has been reported to increase [159,15,158] or decrease with an increased disruption [7,6] for aortic dissections.

Dilatation of the aortic wall secondary to disruptions in elastin organization was reported in a mice study [61]. Although elastin content in the thoracic aortas of patients with an ascending aneurysm (TAV and BAV) decreased compared with control, it was not significantly different between BAV and TAV groups [16,27]. In addition, changes in the elastin architecture of BAV patients compared with TAV were region-specific, and were characterized by a decrease in the number of radially oriented elastin fibers [146]. Primary elastin fiber orientation in the aneurysmatic media of TAV patients changed from longitudinal in the inner part to circumferential in the outer part distinctly in the right lateral region compared with other regions [128].

Similar collagen levels were observed between control and ascending aneurysm samples [61,68,27], and between BAV and TAV phenotypes [104,103,27] contradicting the findings of significantly higher collagen in BAV compared with TAV and control [16]. Regardless, the organization of collagen may still be significantly changed during aneurysm development in the thoracic aorta [7]. Sassani et al. [118] reported notable regional variations in the 2D collagen orientation, with the right lateral and posterior regions having diagonal fibers at smaller angles to the longitudinal axis. On the other hand, Forsell et al. [38] reported similar collagen orientations in aneurysmatic BAV and TAV groups. Phillippi et al. [103] demonstrated that both collagen and elastin fibers in the tangential plane were more aligned in BAV aneurysms and BAV control, and more disorganized in TAV aneurysms compared with TAV control. Percentage of radially oriented elastin and collagen fibers in the outer media was significantly higher in BAV patients and higher in TAV patients compared with control [147].

Abdominal aortic aneurysms (AAAs) typically show increased collagen synthesis at earlier stages, whereas later in the process collagen degradation exceeds its synthesis, and it is accompanied by elastin degradation [125]. The out-of-plane collagen dispersion in AAAs is significantly higher when compared with abdominal aortic tissues, and the characteristic wall structure (with three distinct layers) cannot be identified anymore in AAA samples. In

addition, collagen fibers in the abluminal layer of AAAs loose their waviness and appear as thick straight struts [89].

Several factors in the donor anamnesis may have an influence on the microstructure making it difficult to conclude, for example, which disease is accompanied with which structural changes and at which stages. Nevertheless, the microstructure remains a crucial contributor to mathematical models if one wishes to describe the mechanics and failure.

3. Failure mechanisms involved in dissection and rupture

We now study the load combinations that act on the tissues *in vivo* prior to dissection and rupture, which should be taken care of for a better understanding of tissue failure. In Section 3.1 we start with different theories regarding the loading conditions initiating and propagating the aortic dissections, and continue in Section 3.2 with theories regarding the global and local loading conditions prior to rupture in vehicular trauma. As we will see in the following sections, different loading conditions may lead to similar tissue failure.

3.1. Initiation and propagation of aortic dissection

The study of van Baardwijk & Roach [2] applied pulse pressure to canine thoracic aortas after creating an intimal tear. The authors identified the maximum rate of pressure change $(\mathrm{d}P/\mathrm{d}t)_{\max}$ as the most clearly linked parameter to the propagation of dissection since the crack advanced at the upstroke of the pulse wave. Gaps between the lamellae, as identified during histological investigations, pointed to shearing mechanisms that are responsible for the crack propagation, and the crack typically propagated between adjacent elastic layers. The dissection rate was variable between the pulses, and it was inversely related to the tear depth within the medial layer in contrast to expectations, suggesting heterogeneous wall properties throughout the thickness.

On the other hand, Carson & Roach [13] reported that the medial strength of the porcine aortas does not change with depth under static pressure. The authors stated that the structures linking the lamellae are weaker than the lamellae themselves, resulting in a crack propagation between the lamellae. In addition, the fusion points of the lamellae can force the crack to change the direction. The authors reported quite high pressure values to initiate a bleb, but observed a quick drop in the pressure allowing the dissection to propagate under a physiological load level. A minimum pressure value required for the crack to propagate was not reported therein. Using similar methods to Carson & Roach [13], Tiessen & Roach [141] reported similar results regarding the effect of the tear depth for human aortas, however, the authors noted that the dissection propagated around the plaques instead of going through them. The experiments on porcine aortas performed by Roach & Song [114] showed that although it was much easier to initiate a dissection in the abdominal aorta when compared to the thoracic aorta, the dissections propagated more easily in the thoracic aorta, see Fig. 4. The authors suggested that this is because of structural differences in the elastin pattern between the two sections of the aorta; parallel sheets with fenestrations in the thoracic aorta and a honeycomb-like structure in the abdominal aorta. In a later study, Tam et al. [139] reported that the dissection closer to the adventitial side required a lower pressure to propagate.

The study of Rajagopal et al. [111] suggested hemodynamics together with abnormal mechanical properties, geometry, and the anisotropic wall structure to be important factors for the initiation and the propagation of aortic dissections. The authors proposed that an increased maximum systolic pressure and the mean aortic blood pressure are responsible for the initiation, and an elevated pulse pressure and the heart rate facilitate the propagation. Mikich [83] proposed that the blood flow and the hemorrhage in the media alone cannot cause an initiation and propagation of a dissection, but the process is mainly influenced by smooth muscle cell contraction.

Haslach, Jr. et al. [48] proposed that collagen fiber pullout, during which bonds and filaments attached to the fibers rupture due to shear, is a prerequisite for rupture in circumferential aortic tensile strips and inflated ring specimens. For the longitudinal tensile strips, however, rupture is caused by a peeling mechanism during which the bonds between collagen fibers and the ground matrix rupture. In addition, hydration of the tissue is suggested to play an important role to recover from permanent deformation, loss of which eventually leads to rupture. This research group conducted more ring inflation tests, see Haslach, Jr. et al. [47,49], concluding that, as a result of heterogeneous circumferential deformation, non-negligible circumferential shear stresses could be the reason for the crack propagation in the circumferential- longitudinal plane considering the lamellar structure of the media. Histological investigations of block shear tests showed voids between the collagen bundles, see Fig. 5(a)–(c), possibly resulting from the relative motion of the layers, which can be an indicator of ruptured inter-fiber cross-links [47]. Sommer et al. [131] reported similar observations within in-plane shear tests, as shown in Fig. 5(d), and this mechanism could explain the delaminations observed by Helfenstein-Didier et al. [50] during uniaxial tensile tests, as depicted in Fig. 5(e).

Following the protocol reported by Sugita & Matsumoto [135], recently Sugita & Matsumoto [136] performed biaxial extension tests on thinly sliced porcine thoracic aortas with a reduced cross section in the center and reported a heterogeneous deformation field in terms of strains similar to Sugita & Matsumoto [134]. Strain distribution and the collagen realignment were similar between the crack initiation sites and the remaining tissue sample, in contrast to the idea behind the maximum principal strain failure criterion. Since the collagen density was significantly lower at the crack initiation sites and the cracks propagated along the local collagen fiber direction, the authors suggested that the initiation and propagation of the crack is primarily effected by the collagen architecture. However, anticipated crack initiation at the lowest retardance sites - in other words the sites with the least collagen content - was not observed for all specimens. This suggests that the cross-links between the fibers might also play an important role in the dissection process.

Considering the changes to elastic fibers in aortic dissections and their role in energy dissipation, Chung et al. [19] studied elastic energy loss, defined as the hysteresis divided by the total strain energy. The authors found that an increased elastic energy loss is associated with medial degeneration and with increased collagen to elastin ratio. Furthermore, Chung et al. [18] reported a decrease in the directional differences in energy loss - hence in the degree of anisotropy - in samples with severe medial degeneration. By using newborn mice and genetic engineering to have defects in the elastic fiber structure, Kim et al. [63] suggested

that not only elastin but properly assembled and cross-linked elastic fibers are responsible for a low energy loss in the aorta.

3.2. Traumatic rupture

Blunt aortic trauma typically constitutes a transverse tear in the aortic wall, rarely a longitudinal one (see Fig. 6(a)). The mild degree trauma involves an intramural rupture (laceration), typically leading to a traumatic aortic dissection initiated by a circumferential tear to the intima, which may propagate and lead to complete rupture later in life [62,106]. Severe trauma involves a transmural injury to the aortic wall, which can be in the form of partial, complete, or multiple transections. Fig. 6(b)–(c) shows examples of intramural ruptures with different extents. Multiple ruptures as a combination of intramural and transmural ruptures are also reported in the literature [132,23].

One of the first mechanisms proposed to explain traumatic rupture was the sudden increase in the intraluminal pressure. For example, the shoveling effect - the heart being trapped between the vertebral column, the sternum and the mediastinum due to the compression of the chest and the abdomen - can force the blood from the heart into the aorta suddenly increasing the intraluminal blood pressure [3]. The effect of this pressure increase can be elevated by the cardiac cycle in different ways. For example, Wilson & Roome [161] hypothesized that the aorta is more likely to rupture if an impact to the chest is received at the beginning of diastole since the aorta is completely filled with blood, whereas Marsh & Moore [77] suggested that the deceleration forces acting on the heart during the systole creates a greater risk of rupture of the great vessels at the location of their attachment to the heart. In addition, a phenomenon known as water hammer effect might occur due to the sudden deceleration of the blood in the arch impacting the anterior wall of the aorta and resulting in traction forces on the isthmus region [65,126]. The occlusion of the aortic lumen due viscoelastic effects that decrease the aortic diameter can cause formation of shock waves propagating in the counter-blood flow direction, thereby exerting high axial stresses on the aortic wall and causing a transverse rupture [65].

In addition to the hemodynamic effects, local concentrations of shear stresses may arise due to high deceleration forces [42], the rotation of the first ribs [22], or a combination of rapid deceleration and chest compression [126]. Vertical inertial forces [168], rapid deceleration occurring at different rates at different parts of the body [77,22,126], cranial deceleration [121], the heart being displaced in the thoracic cavity due to inertial effects [153] and the displacement of mediastinal structures [126] can all cause stretching of the aortic wall between fixation points resulting in an injury to the isthmus area due to stress concentrations. Field et al. [37] suggested that traumatic injury does not necessarily follow along the luminal/abluminal direction, considering that some patients did not present an intimal flap. The authors hypothesized that the geometry of the isthmic region in combination with the high number of small branching vessels lead to stress concentrations which are naturally occurring, and the stretching of these vessels may pronounce the effect of inertial or compressive chest loading resulting in intimal rupture, or intramural hematoma.

The above mentioned mechanisms for initiation and propagation of dissection as well as traumatic aortic injury indicate that the cardiac cycle, the blood flow and the geometry of the

aorta together with the aortic attachment points are important factors to consider as they influence the boundary conditions to be imposed on the problem.

4. Tissue strength quantification

Aneurysms rupture when the wall stress exceeds the wall strength. Although it sounds simple, the requirement here is to reliably characterize both the (*in vivo*) stress state of the wall and the (*in vivo*) tissue strength, and neither is trivial. It is inarguably valuable to know how the aortic wall behaves under different loading modes - separated and mixed - to be able to predict the stress state of the wall. However, how much of the stress the tissue can bear at certain loading conditions with a given state of the microstructure remains unknown. As an essential element to a failure criterion framework, the strength quantification needs to be addressed. In this section, we provide an overview of the documented experimental studies quantifying the strength of the aorta in health and disease. We review uniaxial tensile tests performed until failure, bulge inflation and peeling tests and (roughly) summarize related data in the Tables 1–3, respectively. Finally we describe other tests quantifying the tissue strength such as in-plane shear, direct tension and trouser tests. For an illustration of the different tests used to quantify failure properties of aortas see Fig. 7.

4.1. Uniaxial tensile tests performed until rupture

Uniaxial tensile tests have been widely employed to characterize the mechanical properties of aortic tissues. Because of the anisotropic microstructure of the aortic wall, they are typically performed in circumferential and longitudinal directions to obtain direction-dependent properties. The shape of the specimen is either rectangular or (better) bone-shaped, as shown in Fig. 7(a). Table 1 summarizes some of the studies documented in the literature and provides failure stress and stretch values under uniaxial tensile loading. This table is not meant to be a complete summary of all uniaxial rupture tests published in the literature, however, it aims to provide a representative overview and points to the rather large variability in the failure stress and stretch values, also visualized in Fig. 8.

In terms of failure stress the thoracic aortic tissue has been reported to be stronger in the circumferential direction than in the longitudinal direction [85,56,39,104,122,35,131]. However, Vorp et al. [157] observed no significant differences in regard to the testing direction. The study of Mohan & Melvin [85] stated that the longitudinal aortic strength should be more than twice as high as the circumferential strength for the transverse failure to occur. Their quasi-static tests showed no such difference, however, once the strain rates were increased the strength ratios got closer to 1:2. The extension ratios were not effected by the strain rate.

In terms of the ‘yield stress’ the anterior region of AAAs was reported to be the weakest, especially along the longitudinal direction [140] - ‘yield stress’ is here related to the yield point defined as the point on the stress-strain curve where the slope starts to decrease with increasing strain. Failure stresses of anterior, right lateral, posterior and left lateral samples of the ascending aortas were not significantly different for control [56], for aneurysmatic [55,56], and for dissected tissues [72] with respect to the circumferential direction. However, failure stresses in the longitudinal direction were significantly higher in the right lateral

region compared with the anterior and posterior regions [56], but also in the left and right lateral regions compared with the anterior region for aneurysms [55]; and in the right lateral region compared with the left lateral region for dissections [72]. Ferrara et al. [35] reported stronger and stiffer posterior regions with respect to anterior in the circumferential direction for thoracic aortic aneurysms, whereas the opposite trend was observed for the longitudinal direction. Kritharis et al. [68] found similar failure properties in the noncoronary sinuses of the control and aneurysm groups for both young and old patients, whereas failure stresses in the right and left coronary sinus regions were smaller circumferentially and greater longitudinally in aneurysms compared with control.

Although all three layers of ascending thoracic aortic aneurysms exhibited higher failure stresses in the circumferential direction than in the longitudinal direction, the differences were significant only for the media from all regions and for the adventitia from the lateral region [129]. For dissected tissues, failure stresses and stretches were significantly higher in the circumferential than in the longitudinal direction in the inner media at the distal location, but the outer media did not show significant differences regarding the testing direction [72]. Failure stretches of the ascending tissue did not show notable differences between the layers [129,72]. However, failure stresses were significantly higher for the adventitia than for the media and intima for aneurysms [129], and they were significantly higher for the outer media than for the inner media for dissections [72].

Healthy abdominal aortic tissues had significantly higher ultimate strength and yield strength compared to AAAs [110]. Failure tension (for definition see Raghavan et al. [109]) was suggested to be a better predictor of strength than failure stress [109], however, no significant differences were found between ruptured and unruptured AAAs in terms of either parameter [108]. In contrast, circumferential strips of ruptured AAA tissues were reported to have significantly lower failure stresses compared with the unruptured AAA tissue strips by Di Martino et al. [28]. Vorp et al. [156] reported isotropic failure properties for orthogonal strips taken from abdominal aortic aneurysms. Moreover, the failure stress in the longitudinal direction was significantly lower for AAA compared with control. Partially calcified AAA tissue was significantly weaker than the fibrous AAA tissue in terms of the failure stress, stretch and tension [95]. Failure stresses of the AAA wall were also reported to decrease with increasing intraluminal thrombus (ILT) thickness [155,82].

Vorp et al. [157] reported aneurysmatic ascending aortas to have significantly lower failure stresses and stiffer behavior compared to controls. García-Herrera et al. [39] documented no significant differences between the mechanical strength of aneurysmal BAV and aneurysmal TAV aortic specimens, and the corresponding age-matched control group for the ascending aorta. Significantly higher failure stresses were reported in aneurysmatic BAV ascending aortas when compared to aneurysmatic TAV ascending aortas for the intact wall [102,104,38,27,36], and for the media [27]. The failure stretches in two valve phenotypes were similar [102,38], but also significantly higher for BAV than for TAV [27,36]. Histological investigations showed that proportional differences in the tensile strength between BAV and TAV groups cannot be explained by alterations in the elastin content [27] or the collagen content [104,27]. However, the stiffness increase and extensibility reduction in ascending aneurysmatic tissues were associated with a decreased elastin content [128].

In the study of Vande Geest et al. [150] no statistically significant gender-related differences were reported in terms of strength, unlike Sokolis & Iliopoulos [127] who identified that circumferential aneurysmatic specimens obtained from female patients exhibited significantly lower failure stresses compared with the ones obtained from male patients. Furthermore, failure stresses of the aorta are reported to decrease [92,39,68,36], and also the failure stretches [92,68,36] with increasing age. In general, strength was not correlated to diameter [28,55], but it was inversely related to wall thickness [140,28,55].

4.2. Bulge inflation tests

Although uniaxial tensile tests provide valuable insight into the strength characteristics of aortic tissues, they are limited when it comes to representing *in vivo* loading conditions. Methods to quantify tissue strength using planar biaxial tests are not yet developed to the authors' knowledge, therefore, biaxial tests performed via a bulge inflation method, see Fig. 7(b), are the focus of this section. Table 2 summarizes some studies documenting failure stress and (when available) extension to failure, defined in various ways (see the related table).

Aortic specimens failed consistently in the direction perpendicular to the longitudinal axis in bulge inflation tests for human [86] and for porcine tissue [76], and the dynamic biaxial failure pressure was significantly higher than the quasi-static one, 2.14 times [86]. Sugita et al. [137] also documented the normal aorta to be weakest in the longitudinal direction under bulge inflation tests, but there was no dominant crack direction for the aneurysmal tissues. The authors did not observe a persistent rupture initiation at local strain concentration zones in contrast to Kim et al. [64] who reported local strain and stress concentrations at the rupture locations. The study of Kim et al. [64] deduced a stable stress parameter for rupture, quantifying the stress in the direction normal to both families of collagen fibers using the values provided in Table 2. Romo et al. [115] showed that localized thinning of the wall is responsible for rupture and not the location of maximum stress. The related values in Table 2 are the stresses in the direction perpendicular to the crack direction at rupture. Duprey et al. [32] calculated failure stress and stretch similar to Romo et al. [115]. Cracks showed dissection-like properties, where the media and the intima failed first creating a sudden drop in the stress curves, but the adventitia was still able to carry (some) load. The authors found no significant differences between BAV and TAV patients, whereas age had a significant impact on the failure properties. In addition, they reported no correlation between the aneurysm diameter and the failure stress/stretch. Luo et al. [70] investigated the elastic properties, direction of maximum stiffness, stress, strain, and the energy consumption at the rupture sites of 9 aneurysmatic ascending aortic samples. The authors reported the tissues to consistently fail in the direction of maximum stiffness and highest energy, indicating that higher stiffness does not mean higher strength. Since high stiffness and energy values mean more collagen recruitment, they concluded that collagen fibers must play a significant role in the rupture process.

Pearson et al. [100] found no significant differences in rupture pressure between the ascending, descending, and isthmus regions. However, they reported significantly larger extension to failure in the ascending aortic samples compared to the isthmus samples, which

is in contrast to Marra et al. [76] who found no significant influence of the aortic location on the axial failure stress or stretch. Histological investigations in Pearson et al. [100] showed isthmus samples to have a higher collagen to elastin ratio, likely making the samples from this region less extensible. The failure stresses were significantly larger for the descending aorta than for the isthmus region, however, the overlap in the data between the isthmus and the adjacent regions let the authors conclude that the mechanical failure properties cannot account for the clinical observations pointing to the isthmus as a primary injury location.

4.3. Peeling tests

As mentioned above, the propagation of the dissection is mainly attributed to the lamellar structure of the aortic wall. Peeling tests, which is not the sole appropriate method, can provide us with the delamination strength of the wall at different locations. The ‘strength’ of the wall is typically quantified in terms of force per width (F/w) and the dissection energy (W_{diss}). On the basis of some studies Table 3 provides an overview of these values for the aorta, and Fig. 7(c) shows a sketch of a peeling test.

Higher force per width for axial strips compared to circumferential strips of the abdominal aortic media was reported by Sommer et al. [130] - note that this difference was not significant. Furthermore, the authors observed that the damage was spread over six to seven lamellae. Fig. 9(a) and (b) depicts the histological sections of circumferential and longitudinal strips under peeling. Pasta et al. [99] investigated the dissection properties of human ascending aortas in aneurysmal BAV and TAV patients. Compared to the control group, both aneurysm groups required significantly lower force per width, where the TAV group was significantly stronger than the BAV group. The controls showed a strong anisotropy, where the axial direction was significantly stronger, which was not observed in neither aneurysm group. Scanning electron microscopy investigation showed a larger number of ruptured elastin fibers, which is in accordance with the fiber bridging failure mode, see Fig. 9(c).

Kozuń [66] showed that the dissection properties are direction dependent also for stage II atherosclerotic aortas (classification according to Stary [133]), in particular the force per width F/w and the dissection energy W_{diss} were higher in the longitudinal direction. In addition, a significantly higher dissection energy W_{diss} for the adventitia/media + intima (A-MI) interface compared to the adventitia + media/intima (AM-I) interface was reported. Following Kozuń [66], Kozuń[67] found the dissection energy for A-MI and AM-I interfaces in both circumferential and longitudinal directions to decrease with later stages of atherosclerosis (classification according to Stary [133]) until stage IV, whereas stages V and VI were characterized by an increase in the energy. Tong et al. [143] reported a decreased dissection energy for the media/intima (MI) composite as well as a decreased anisotropy with increasing ILT age. In addition to the values provided in Table 3, the authors performed peeling tests on the ILT. Histological investigations showed smooth peeling surfaces in the ILT due to single fibrin fibers or smaller protein clots within the ILT. In addition, the elastin content in the wall decreased as the thrombus age increased, whereas the collagen content did not change signifycantly. The authors reported a rate-dependent change in the dissection properties of both the ILT and the ILT-covered wall. Noble et al. [90] analyzed the influence

of collagenase, elastase, and glutaraldehyde treatment on the dissection properties of porcine thoracic aortas. Collagenase significantly decreased the resistance to dissection, whereas glutaraldehyde increased it and elastase had no significant effect. In terms of anisotropy, their results were similar to Sommer et al. [130].

4.4. Other tests quantifying tissue strength

Trouser tests, as illustrated in Fig. 7(d), in addition to uniaxial tensile tests, were performed on porcine descending thoracic aortas by Purslow [107]. The author reported that the longitudinal direction is more resistant to tearing than the circumferential direction, such that some longitudinal test samples showed cracks that deviated to the circumferential direction making data from these tests unusable for further analysis. In addition, the author found that the circumferential toughness increased with increasing distance from the heart. The study of Chu et al. [17] showed that the stiffness and the fracture toughness of aortas decreased with increasing fatigue by using cyclic loading tests followed by biaxial and guillotine tests. On the basis of the guillotine method documented by Chu et al. [17], Shahmansouri et al. [123] used a custom-made toughness-tester apparatus for tests on control and aneurysmatic ascending aortic tissues taken from four quadrants, and the authors measured the circumferential toughness and the incremental elastic modulus at 10% Green-Lagrange strain. Neither parameter showed regional dependency, however, both correlated well with the total amount of structural proteins (collagen and elastin). More specifically, the toughness decreased with increasing collagen content. The average toughness was not correlated with the average circumferential or longitudinal moduli.

Curves of direct tension tests (see Fig. 7(e)) on abdominal aortas [130] and thoracic aortas [131] showed three characteristic regions, namely elastic, damage, and failure. The average radial failure stress for human abdominal aortas was 140.1 ± 15.9 kPa and for diseased human thoracic aortas 131 ± 56 kPa. Comparing these values with the data from uniaxial tests in Table 1, it is clear that the aorta is weakest in terms of the failure stress under radial loading due to its lamellar structure, as also pointed out by MacLean et al. [71], see Fig. 2.

In-plane and out-of-plane shear tests until failure in circumferential and longitudinal directions were performed on diseased human thoracic aortas by Sommer et al. [131]. The sheared plane and the direction of shearing during an in-plane shear test is depicted in Fig. 7(f). Out-of-plane shear strength was almost 10-fold higher compared to the in-plane shear strength, which is a result of the lamellar structure and the collagen architecture of the aorta. The shear-lap test results of Witzenburg et al. [163] were similar to the in-plane shear tests of [131], although the geometry of the samples were slightly different. The authors reported that circumferential samples exhibited significantly higher peak stresses (nominal) than longitudinal samples.

5. Biomechanically motivated models to predict rupture risk

There may be different reasons for the similar locations at which traumatic injuries and the initiation of aortic dissections occur, as pointed out in the introduction. One reason may be that since the aorta is attached to the left pulmonary artery by the ligamentum arteriosum at the isthmus and to the vertebral column by the fascia, it cannot deform as extensively as

other locations leading to local stress concentrations. Another reason may be that the aortic wall has an inherently different strength in these locations due to its microstructure, e.g., due to differences in collagen and elastin content, orientation, or cross-linking proteins. Since the aorta may be subjected to stress concentrations and has heterogeneous strength distributions along the tree, stress and strength are frequently used in models to predict rupture risk. Next we summarize a few existing models designed to evaluate the risk of rupture.

Doyle et al. [31,30] performed inflation tests on silicone rubber to mimic the inflation of abdominal aortic aneurysms (AAA), and observed rupture at the regions of inflections instead of maximum diameter. They also reported rupture at peak stress locations in 80% of the cases using computational models. Nathan et al. [88] performed finite element analyses on 47 normal thoracic aortic geometries by assuming that the aortic wall is homogeneous, incompressible, isotropic and linearly elastic, a rather rough assumption. The results showed that the mean wall peak stresses occurred above the sinotubular junction (0.43 ± 0.07 MPa) and distal to the left subclavian artery (0.21 ± 0.07MPa), which is in line with the common locations of dissection initiation. This led to the conclusion that the stress distribution is the main contributor to the dissection process. Biaxial extension tests on aneurysmatic ($n = 18$) and healthy ($n = 19$) ascending aortic samples showed that aneurysmatic samples are much stiffer under physiological loading conditions [1]. Hence, the authors suggested that the patient-specific wall stress could be a good predictor of rupture risk. The study did not find any correlation between the maximum diameter and the patient-specific stress levels. Addressing the large variations in strength and the uncertainties in wall stress predictions, Polzer & Gasser [105] developed a probabilistic rupture risk index (PRRI), calculated by using the wall strength and the peak stress distribution. The authors were able to distinguish between the intact and ruptured AAA cases. PRRI values were strongly correlated with the mean arterial pressure, but not with the maximum diameter.

On the basis of heterogeneous strength distribution in aneurysm walls, Vallabhaneni et al. [149] suggested that the locations with increased enzymatic activity within the wall could be responsible for a local weakening making the aneurysm more prone to rupture. Vande Geest et al. [151,152] reported different statistical risk prediction models considering the heterogeneity of both the wall stress and the wall strength. Simulations using the model of Vande Geest et al. [151] indicated that the unruptured AAAs had significantly higher failure stresses compared to the ruptured group. Even though this model could not be validated by Reeps et al. [112], it involves a non-invasive estimation of patient-specific wall strength, and it was used by Joldes et al. [60] to develop a rupture risk calculation software. The approach of Joldes et al. [60] eliminates the need to use patient-specific material parameters as the stresses are only determined by the external load and the geometry, depending only weakly on the material parameters (for a detailed discussion see Wittek et al. [162], Lu [84], Joldes et al. [59]).

Trabelsi et al. [144] compared three different rupture risk assessment methods, in particular, maximum diameter, rupture risk index, and the overpressure index (see definitions therein). The maximum diameter criterion was only weakly correlated with the other two, and, remarkably, the patient with the smallest aneurysm diameter had the highest rupture risk index. Duprey et al. [32] suggested a rupture risk criterion for aneurysms of ascending aortas

based on a maximum stretch parameter γ_{stretch} the authors introduced. It indicates that the failure is reached when the stretch acting on the tissue is larger than its maximum extensibility. The data obtained via bulge inflation tests therein showed a strong correlation between γ_{stretch} and the physiological elastic modulus. Trabelsi et al. [145] were able to further correlate this rupture risk indicator with the membrane stiffness using the analysis of CT-scans, concluding that the loss of elasticity increases the rupture risk. However, the authors stated that the correlation was not strong enough for this criterion to be suggested for use in clinical practice.

Martin et al. [80] quantified the rupture diameter risk and the yield diameter risk defined as the diameter D_{sys} at systolic pressure divided by the diameter D_{f} at rupture pressure ($D_{\text{sys}}/D_{\text{f}}$) and by the diameter D_{y} at yield pressure ($D_{\text{sys}}/D_{\text{y}}$), respectively. Both risk indicators were related with increases in the clinically measured parameters such as systolic blood pressure, age, systolic wall tension and pressure-strain modulus (rupture diameter risk was additionally correlated with the aortic size index; for the related definition see Davies et al. [25]), but not with the aneurysm diameter. Building on this framework, Martin et al. [79] performed patient-specific finite element analyses using geometries reconstructed from CT scans and clinical blood pressure measurements, in addition to mechanical data from these aortas reported previously by Pham et al. [102]. The rupture diameter risk was correlated with the simulated peak wall stresses and with the tension-strain modulus, but not with the systolic hoop tension and the overall aneurysm diameter. The predicted rupture pressures decreased dramatically with increasing rupture diameter risk.

6. Concluding remarks

Despite the advances in medical, biomedical and biomechanical research, the mortality rates of dissections and aortic aneurysms remain high. The present review article summarizes experimental studies that quantify the aortic wall strength and it discusses biomechanically motivated models to predict rupture risk. Following the description of the aortic microstructure and the pathological changes leading to dissection and aneurysm in Section 2, we summarized experimental investigations that were designed to better understand failure mechanisms involved in dissection and rupture in Section 3. In the case of aortic trauma, we have seen in Section 3.2 that there may be different global load cases on, e.g., the chest resulting in a similar load on the aortic wall leading to a similar material failure. As suggested by Richens et al. [113], multivariate hypotheses are more suitable to explain under what loading conditions the aorta ruptures. Such hypotheses can bring the global mechanisms together, i.e. shearing, torsion and stretching, and suggest which stresses play a more pronounced role during rupture. Various loads acting on the aortic wall prior to rupture call for the strength identification under different loading modes.

In Section 4 we focused on uniaxial tensile, bulge inflation and peeling tests while briefly touching upon trouser, direct tension and shear tests. We identified contradictory observations and a large variation within and between data sets, which may be due to biological variations, different sample sizes, differences in experimental protocols, etc. However, we pointed to the underlying structural similarities/differences as the main contributor to the similarities/differences of the strength values. Considering the pathological

microstructural changes, aneurysmatic and dissected tissues are expected to exhibit different strength properties compared to control tissues although this is not always the case according to the mechanical test results, as pointed out in Section 4. However, it seems that the micro-architecture, in particular the content and organization of collagen and elastin and their cross-linking proteins play an important role during failure.

Finally, in Section 5 we looked at what is proposed in the literature to predict the risk of rupture as an alternative to the maximum diameter criterion. Realistic geometries and appropriate constitutive models are crucial to identify wall stresses and zones of stress concentration. Martufi & Gasser [81] elaborated on a wall-averaged stress state (membrane stress state) to be a more realistic AAA rupture risk indicator, also pointing out the importance of using appropriate constitutive models to predict wall stresses. As mentioned before and addressed by several risk prediction models, not only the stress state at a point in time but also the strength distribution is likely to be heterogeneous. Although rupture risk prediction models address an important issue in clinical practice, they do not model material failure.

Let us finally consider a few more recent findings on tissue failure. Converse et al. [21] showed that ‘arterial yielding’ was closely correlated with the onset of collagen damage, which is indicated by the binding of collagen hybridizing peptide to undulated collagen [169]. In addition, damage accumulation increased with increasing stretch beyond the ‘yield threshold’, and it occurred primarily in the fibers along the loading direction [21]. This suggests that orientation and dispersion of collagen determine the strength of, e.g., aortic tissues [124] and the pericardium [160]. Marino et al. [74] proposed a damage model considering interstrand delaminations as a source of inelastic deformation, as suggested by multiscale models of collagen fibrils [75,73] and by atomistic computations [10,148]. Employing the experimental protocols documented in Converse et al. [21], Marino et al. [74] showed that damage onset and excessive damage accumulation agree well with the predicted evolution of the model parameters that describe tissue softening associated with permanent molecular elongation, and tissue failure associated with loss of fibril structural integrity.

More advanced failure criteria for fibrous biological tissues are of pressing need to better understand aneurysm rupture and propagation of aortic dissections, and to substantially improve clinical decision making; should also go hand in hand with developments in clinical biomarkers and/or suitable imaging modalities. In the light of this review, we suggest that an ideal failure criterion should include the strength of the material under different loading cases and the effect of the tissue microstructure on the strength at different length scales. In particular, a failure criterion should be based on microstructural properties including the content and organization of remodeled collagen and remnant elastin and their cross-linking proteins, especially under the influence of proteolytic activity. Such failure criteria may also improve G&R models necessary of addressing the key issue of rupture-potential.

Acknowledgement

We would like to acknowledge Yutaka Nakashima from the Division of Pathology, Japanese Red Cross Fukuoka Hospital in Japan and Justyna A. Niestrawska from the Institute of Biomechanics, Graz University of Technology in Austria for providing the two images of the microstructure of the aortic dissection and the aneurysm, as presented in

the graphical abstract. In addition, we gratefully acknowledge the aneurysm image, also presented in the graphical abstract, which we received from Erasmo Simão da Silva from the Division of Vascular and Endovascular Surgery, University of São Paulo in Brazil and Madhavan L. (Suresh) Raghavan from the Department of Biomedical Engineering, University of Iowa, Iowa City, USA. This work was partly supported by the Lead Project on 'Mechanics, Modeling and Simulation of Aortic Dissection', granted by Graz University of Technology, Austria. Furthermore, we gratefully acknowledge the financial support of the National Institutes of Health (NIH), research Grant No. NIH R01HL117063.

References

[1]. Azadani AN, Chitsaz S., Mannion A., Mookhoek A., Wisneski A., Guccione JM, Hope JM, Ge MD, Tseng EE, Biomechanical properties of human ascending thoracic aortic aneurysms, Ann. Thorac. Surg. 96 (2013) 50–58. [PubMed: 23731613]

[2]. van Baardwijk C., Roach MR, Factors in the propagation of aortic dissection in canine thoracic aortas, J. Biomech. 20 (1987) 67–73. [PubMed: 3558430]

[3]. Ben-Menachem Y., Handel S., Angiography in Trauma: A Work Atlas, WB Saunders, 1981.

[4]. Bertrand S., Cuny S., Petit P., Trosseille X., Page Y., Guillemot H., Drazetic P., Traumatic rupture of thoracic aorta in real-world motor vehicle crashes, Traffic Inj. Prev. 9 (2008) 153–161. [PubMed: 18398779]

[5]. Bode-Jänisch S., Schmidt A., Günther D., Stuhrmann M., Fieguth A., Aortic dissecting aneurysms - histopathological findings, Forensic. Sci. Int. 214 (2012) 13–17. [PubMed: 21794994]

[6]. Borges LF, Blini JPF, Dias RR, Gutierrez PS, Why do aortas cleave or dilate? Clues from an electronic scanning microscopy study in human ascending aortas, J. Vasc. Res. 51 (2014) 50–57. [PubMed: 24335355]

[7]. Borges LF, Jaldin RG, Dias RR, Stolf NA, Michel JB, Gutierrez PS, Collagen is reduced and disrupted in human aneurysms and dissections of ascending aorta, Hum. Pathol. 39 (2008) 437–443. [PubMed: 18261628]

[8]. Borges LF, Touat Z., Leclercq A., Zen AA, Jondeau' G., Franc B., Philippe M., Melihac O., Gutierrez PS, Michel J., Tissue diffusion and retention of metalloproteinases in ascending aortic aneurysms and dissections, Hum. Pathol. 40 (2009) 306–313. [PubMed: 18973916]

[9]. Brownstein AJ, Ziganshin BA, Elefteriades JA, Human aortic aneurysm genomic dictionary: is it possible? Indian, J. Thorac. Cardiovasc. Surg. (2018). doi:10.1007/s12055-018-0659-6.

[10]. Buehler MJ, Nanomechanics of collagen fibrils under varying cross-link densities: Atomistic and continuum studies, J. Mech. Behav. Biomed. Mater. 1 (2008) 59–67. [PubMed: 19627772]

[11]. Campa JS, Greenhalgh RM, Powell JT, Elastin degradation in abdominal aortic aneurysms, Atherosclerosis 65 (1987) 13–21. [PubMed: 3649236]

[12]. Canham PB, Finlay HM, Dixon JG, Boughner DR, Chen A., Measurements from light and polarised light microscopy of human coronary arteries fixed at distending pressure, Cardiovasc. Res. 23 (1989) 973–982. [PubMed: 2611805]

[13]. Carson MW, Roach MR, The strength of the aortic media and its role in the propagation of aortic dissection, J. Biomech. 23 (1990) 579–588. [PubMed: 2341419]

[14]. Cherif H., Gogly B., Loison-Robert L-S, Couty L., Ferré FC, Nassif A., Lafont A., Fournier BPJ, Comparative study of abdominal and thoracic aortic aneurysms: their pathogenesis and a gingival fibroblasts-based ex vivo treatment, Springerplus 4 (2015) 231. [PubMed: 26110102]

[15]. Cheuk BLY, Cheng SWK, Differential expression of elastin assembly genes in patients with Stanford Type A aortic dissection using microarray analysis, J. Vasc. Surg. 53 (2011) 1071–1078. [PubMed: 21276682]

[16]. Choudhury N., Bouchot O., Rouleau L., Tremblay D., Cartier R., Butany J., Mongrain R., Leask RL, Local mechanical and structural properties ofhealthyand diseased human ascending aorta tissue, Cardiovasc. Pathol. 18 (2009) 83–91. [PubMed: 18402840]

[17]. Chu B., Gaillard E., Mongrain R., Reiter S., Tardif JC, Characterization of fracture toughness exhaustion in pig aorta, J. Mech. Behav. Biomed. Mater. 17 (2013) 126–136. [PubMed: 23122712]

[18]. Chung J., Lachapelle K., Cartier R., Mongrain R., Leask RL, Loss of mechanical directional dependency of the ascending aorta with severe medial degeneration, Cardiovasc. Pathol. 26 (2017) 45–50. [PubMed: 27888778]

[19]. Chung J., Lachapelle K., Wener E., Cartier R., De Varennes B., Fraser R., Leask RL, Energy loss, a novel biomechanical parameter, correlates with aortic aneurysm size and histopathologic findings, J. Thorac. Cardiovasc. Surg. 148 (2014) 1082–1089. [PubMed: 25129601]

[20]. Cikach FS, Koch CD, Mead TJ, Galatioto J., Willard BB, Emerton KB, Eagleton MJ, Blackstone EH, Ramirez F., Roselli EE, Apte SS, Massive aggrecan and versican accumulation in thoracic aortic aneurysm and dissection, JC I Insight 3 (2018) e97167.

[21]. Converse MI, Walther RG, Ingram JT, Li Y., Yu SM, Monson KL, Detection and characterization of molecular-level collagen damage in overstretched cerebral arteries, Acta Biomater. 67 (2018) 307–318. [PubMed: 29225149]

[22]. Crass JR, Cohen AM, Motta AO, Tomashefski JF Jr, Wiesen EJ, A proposed new mechanism of traumatic aortic rupture: the osseous pinch, Radiology 176 (1990) 645–649. [PubMed: 2389022]

[23]. Creasy JD, Chiles C., Routh WD, Dyer RB, Overview of traumatic injury of the thoracic aorta, Radiographics 17 (1997) 27–45. [PubMed: 9017797]

[24]. Criado FJ, Aortic dissection: a 250-year perspective, Tex. Heart Inst. J. 38 (2011)694–700. [PubMed: 22199439]

[25]. Davies RR, Gallo A., Coady MA, Tellides G., Botta DM, Burke B., Coe MP, Kopf GS, Elefteriades JA, Novel measurement of relative aortic size predicts rupture of thoracic aortic aneurysms, Ann. Thorac. Surg. 81 (2006) 169–177. [PubMed: 16368358]

[26]. Davies RR, Goldstein LJ, Coady MA, Tittle SL, Rizzo JA, Kopf GS, Elefteriades JA, Yearly rupture or dissection rates for thoracic aortic aneurysms: simple prediction based on size, Ann. Thorac. Surg. 73 (2002) 17–27. [PubMed: 11834007]

[27]. Deveja RP, Iliopoulos DC, Kritharis EP, Angouras DC, Sfyris D., Papadodima SA, Sokolis DP, Effect of aneurysm and bicuspid aortic valve on layer-specific ascending aorta mechanics, Ann. Thorac. Surg. 106 (2018) 1692–1701. [PubMed: 29964022]

[28]. Di Martino ES, Bohra A., Vande Geest JP, Gupta NY, Makaroun MS, Vorp DA, Biomechanical properties of ruptured versus electively repaired abdominal aortic aneurysm wall tissue, J. Vasc. Surg. 43 (2006) 570–576. [PubMed: 16520175]

[29]. Dingemans KP, Teeling P., Lagendijk JH, Becker AE, Extracellular matrix of the human aortic media: an ultrastructural histochemical and immunohistochemical study of the adult aortic media, Anat. Rec. 258 (2000) 1–14. [PubMed: 10603443]

[30]. Doyle BJ, Cloonan AJ, Walsh MT, Vorp DA, McGloughlin TM, Identification of rupture locations in patient-specific abdominal aortic aneurysms using experimental and computational techniques, J. Biomech. 43(2010)1408–1416. [PubMed: 20152982]

[31]. Doyle BJ, Corbett TJ, Callanan A., Walsh MT, Vorp DA, McGloughlin TM, An experimental and numerical comparison of the rupture locations of an abdominal aortic aneurysm, J. Endovasc. Ther. 16 (2009) 322–335. [PubMed: 19642790]

[32]. Duprey A., Trabelsi O., Vola M., Favre JP, Avril S., Biaxial rupture properties of ascending thoracic aortic aneurysms, Acta Biomater. 42 (2016) 273–285. [PubMed: 27345137]

[33]. Elefteriades JA, Thoracic aortic aneurysm: reading enemy's playbook, YaleJ. Biol. Med. 81 (2008) 175–186.

[34]. Erdheim J., Medionecrosis aortae idiopathica, Virch. Arch. Pathol. Anat. 273 (1929) 454–479.

[35]. Ferrara A., Morganti S., Totaro P., Mazzola A., Auricchio F., Human dilated ascending aorta: mechanical characterization via uniaxial tensile tests, J. Mech. Behav. Biomed. Mater. 53 (2016) 257–271. [PubMed: 26356765]

[36]. Ferrara A., Totaro P., Morganti S., Auricchio F., Effects of clinico-pathological risk factors on in-vitro mechanical properties of human dilated ascending aorta, J. Mech. Behav. Biomed. Mater. 77 (2018) 1–11. [PubMed: 28886508]

[37]. Field ML, Sastry P., Zhao AR, Richens D., Small vessel avulsion and acute aortic syndrome: a putative aetiology for initiation and propagation of blunt traumatic aortic injury at the isthmus, Med. Hypotheses 68 (2007) 1392–1398. [PubMed: 17196753]

[38]. Forsell C., Bjorck HM, Eriksson P., Franco-Cereceda A., Gasser TC, Biomechanical properties of the thoracic aneurysmal wall: differences between bicuspid aortic valve and tricuspid aortic valve patients, Ann. Thorac. Surg. 98 (2014) 65–71. [PubMed: 24881863]

[39]. García-Herrera CM, Atienza JM, Rojo FJ, Claes E., Guinea GV, Celentano DJ, García-Montero C., Burgos RL, Mechanical behaviour and rupture of normal and pathological human ascending aortic wall, Med. Biol. Eng. Comput. 50 (2012) 559–566. [PubMed: 22391945]

[40]. Gasser TC, Ogden RW, Holzapfel GA, Hyperelastic modelling of arterial layers with distributed collagen fibre orientations, J.R. Soc. Interface 3 (2006) 15–35. [PubMed: 16849214]

[41]. Goldfinger JZ, Halperin JL, Marin ML, Stewart AS, Eagle KA, Fuster V., Thoracic aortic aneurysm and dissection, J. Am. Coll. Cardiol. 64 (2014) 1725–1739. [PubMed: 25323262]

[42]. Greendyke RM, Traumatic rupture of aorta, J. Am. Med. Assoc. 195 (1966) 527–530.

[43]. Grootenboer N., Bosch JL, Hendriks JM, van Sambeek MR, Epidemiology, aetiology, risk of rupture and treatment of abdominal aortic aneurysms: does sex matter?, Eur J. Vasc. Endovasc. Surg. 38 (2009) 278–284. [PubMed: 19540779]

[44]. Gültekin O., Holzapfel GA, A brief review on computational modeling of rupture in soft biological tissues. Computational methods in applied sciences, in: Oñate O., Peric D., de Souza Neto E., Chiumenti M. (Eds.), Advances in Computational Plasticity, A Book in Honour of D. Roger J. Owen, vol. 46, Springer Nature, 2018, pp. 113–144.

[45]. Hans SS, Jareunpoon O., Balasubramaniam M., Zelenock GB, Size and location of thrombus in intact and ruptured abdominal aortic aneurysms, J. Vasc. Surg. 41 (2005) 584–588. [PubMed: 15874920]

[46]. Harvey JG, Gough MH, A comparison of the traumatic effects of vascular clamps, Br. J. Surg. 68 (1981) 267–272. [PubMed: 7225742]

[47]. Haslach HW Jr., Leahy LN, Fathi P., Barrett JM, Heyes AE, Dumsha TA, McMahon EL, Crack propagation and its shear mechanisms in the bovine descending aorta, Cardiovasc. Eng. Technol. 6 (2015) 501–518. [PubMed: 26577482]

[48]. Haslach HW Jr., Riley P., Molotsky A., The influence of medial substructures on rupture in bovine aortas, Cardiovasc. Eng. Technol. 2 (2011) 372–387.

[49]. Haslach HW Jr., Siddiqui A., Weerasooriya A., Nguyen R., Roshgadol J., Monforte N., McMahon E., Fracture mechanics of shear crack propagation and dissection in the healthy bovine descending aortic media, Acta Biomater. 68 (2018) 53–66. [PubMed: 29292167]

[50]. Helfenstein-Didier C., Taïnoff D., Viville J., Adrien J., Maire É., Badel P., Tensile rupture of medial arterial tissue studied by X-ray micro-tomography on stained samples, J. Mech. Behav. Biomed. Mater. 78 (2018) 362–368. [PubMed: 29207329]

[51]. Henson GF, Rob CG, A comparative study of the effects of different arterial clamps on the vessel wall, Br. J. Surg. 43 (1956) 561–564. [PubMed: 13342412]

[52]. Holzapfel GA, Fereidoonnezhad B., Modeling of damage in soft biological tissues, in: Payan Y., Ohayon J. (Eds.), Biomechanics of Living Organs. Hyperelastic Constitutive Laws for Finite Element Modeling, Academic Press, 2017, pp. 101–123.

[53]. Holzapfel GA, Gasser TC, Ogden RW, A new constitutive framework for arterial wall mechanics and a comparative study of material models, J. Elasticity 61 (2000) 1–48.

[54]. Humphrey JD, Holzapfel GA, Mechanics, mechanobiology, and modeling of human abdominal aorta and aneurysms, J. Biomech. 45 (2012) 805–814. [PubMed: 22189249]

[55]. Iliopoulos DC, Deveja RP, Kritharis EP, Perrea D., Sionis GD, Toutouzas K., Stefanadis C., Sokolis DP, Regional and directional variations in the mechanical properties of ascending thoracic aortic aneurysms, Med. Eng. Phys. 31 (2009) 1–9. [PubMed: 18434231]

[56]. Iliopoulos DC, Kritharis EP, Giagini AT, Papadodima SA, Sokolis DP, Ascending thoracic aortic aneurysms are associated with compositional remodeling and vessel stiffening but not weakening in age-matched subjects, J. Thorac. Cardiovasc. Surg. 137 (2009) 101–109. [PubMed: 19154911]

[57]. Isselbacher EM, Thoracic and abdominal aortic aneurysms, Circulation 111 (2005) 816–828. [PubMed: 15710776]

[58]. Jameson JL, Fauci AS, Kasper DL, Hauser SL, Longo DL, Loscalzo J., Harrison's Principle of Internal Medicine, 20th ed, McGraw-Hill Education, 2018.

[59]. Joldes GR, Miller K., Wittek A., Doyle B., A simple, effective and clinically applicable method to compute abdominal aortic aneurysm wall stress, J. Mech. Behav. Biomed. Mater. 58 (2016) 139–148. [PubMed: 26282385]

[60]. Joldes GR, Miller K., Wittek A., Forsythe R., Newby DE, Doyle BJ, BioPARR: a software system for estimating the rupture potential index for abdominal aortic aneurysms, Sci. Rep. 7 (2017) 4641. [PubMed: 28680081]

[61]. Jones JA, Beck C., Barbour JR, Zavadzkas JA, Mukherjee R., Spinale FG, Ikonomidis JS, Alterations in aortic cellular constituents during thoracic aortic aneurysm development: myofibroblast-mediated vascular remodeling, Am.J. Pathol. 175 (2009) 1746–1756. [PubMed: 19729479]

[62]. Keen G., Closed injuries of the thoracic aorta, Ann. Roy. Coll. Surg. Engl. 51 (1972) 137–156. [PubMed: 5086055]

[63]. Kim J., Staiculescu MC, Cocciolone AJ, Yanagisawa H., Mecham RP, Wagenseil JE, Crosslinked elastic fibers are necessary for low energy loss in the ascending aorta, J. Biomech. 61 (2017) 199–207. [PubMed: 28778385]

[64]. Kim JH, Avril S., Duprey A., Favre JP, Experimental characterization of rupture in human aortic aneurysms using a full-field measurement technique, Biomech. Model. Mechanobiol. 11 (2012) 841–853. [PubMed: 22048330]

[65]. Kivity Y., Collins R., Nonlinear wave propagation in viscoelastic tubes: application to aortic rupture, J. Biomech. 7 (1974) 67–76. [PubMed: 4820653]

[66]. Kozuń M., Delamination properties of the human thoracic arterial wall with early stage of atherosclerosis lesions, J. Theor. Appl. Mech. 54 (2016) 229–238.

[67]. Kozuń M., Kobielarz M., Chwiikowska A., Pezowicz C., The impact of development of atherosclerosis on delamination resistance of the thoracic aortic wall, J. Mech. Behav. Biomed. Mater. 79 (2018) 292–300. [PubMed: 29353772]

[68]. Kritharis EP, Iliopoulos DC, Papadodima SA, Sokolis DP, Effects of aneurysm on the mechanical properties and histologic structure of aortic sinuses, Ann. Thorac. Surg. 98 (2014) 72–79. [PubMed: 24811985]

[69]. Lederle FA, Wilson SE, Johnson GR, Reinke DB, Littooy FN, Acher CW, Ballard DJ, Messina LM, Gordon IL, Chute EP, Krupski WC, Busuttil SJ, Barone GW, Sparks S., Graham LM, Rapp JH, Makaroun MS, Moneta GL, Cambria RA, Makhoul RG, Eton D., Ansel HJ, Freischlag JA, Bandyk D., Aneurysm Detection and Management Veterans Affairs Cooperative Study Group, Immediate repair compared with surveillance of small abdominal aortic aneurysms, N. Engl. J. Med. 346 (2002) 1437–1444. [PubMed: 12000813]

[70]. Luo Y., Duprey A., Avril A., Lu J., Characteristics of thoracic aortic aneurysm rupture in vitro, Acta Biomater. 42 (2016) 286–295. [PubMed: 27395826]

[71]. MacLean NF, Dudek NL, Roach MR, The role of radial elastic properties in the development of aortic dissections, J. Vasc. Surg. 29 (1999) 703–710. [PubMed: 10194499]

[72]. Manopoulos C., Karathanasis I., Kouerinis I., Angouras DC, Lazaris A., Tsangaris S., Sokolis DP, Identification of regional/layer differences in failure properties and thickness as important biomechanical factors responsible for the initiation of aortic dissections, J. Biomech. 80 (2018) 102–110. [PubMed: 30195853]

[73]. Marino M., Molecular and intermolecular effects in collagen fibril mechanics: a multiscale analytical model compared with atomistic and experimental studies, Biomech. Model. Mechanobiol. 15 (2016) 133–154. [PubMed: 26220454]

[74]. Marino M., Converse MI, Monson KL, Wriggers P., Molecular-level collagen damage explains softening and failure of arterial tissues: a quantitative interpretation of CHP data with a novel elasto-damage model, J. Mech. Behav. Biomed. Mater. 97 (2019) 254–271. [PubMed: 31132662]

[75]. Marino M., Vairo G., Influence of inter-molecular interactions on the elasto-damage mechanics of collagen fibrils: a bottom-up approach towards macroscopic tissue modeling, J. Mech. Phys. Solids 73 (2014) 38–54.

[76]. Marra SP, Kennedy FE, Kinkaid JN, Fillinger MF, Elastic and rupture properties of porcine aortic tissue measured using inflation testing, Cardiovasc. Eng. 6 (2006) 125–133.

[77]. Marsh CL, Moore RC, Deceleration trauma, Am. J. Surg. 93 (1957) 623–631. [PubMed: 13403097]

[78]. Marshall TK, Traumatic dissecting aneurysms, J. Clin. Pathol. 11 (1958) 36–39. [PubMed: 13502458]

[79]. Martin C., Sun W., Elefteriades J., Patient-specific finite element analysis of ascending aorta aneurysms, Am. J. Physiol. Heart Circ. Physiol. 308 (2015) H1306–H1316. [PubMed: 25770248]

[80]. Martin C., Sun W., Pham T., Elefteriades J., Predictive biomechanical analysis of ascending aortic aneurysm rupture potential, Acta Biomater. 9 (2013) 9392–9400. [PubMed: 23948500]

[81]. Martufi G., Gasser TC, Review: the role of biomechanical modeling in the rupture risk assessment for abdominal aortic aneurysms, J. Biomech. Eng. 135 (2013) 021010.

[82]. Martufi G., Satriano A., Moore RD, Vorp DA, Di Martino ES, Local quantification of wall thickness and intraluminal thrombus offer insight into the mechanical properties of the aneurysmal aorta, Ann. Biomed. Eng. 43 (2015) 1759–1771. [PubMed: 25631202]

[83]. Mikich M., Dissection of the aorta: a new approach, Heart 89 (2003) 6–8. [PubMed: 12482778]

[84]. Miller K., Lu J., On the prospect of patient-specific biomechanics without patient-specific properties of tissues, J. Mech. Behav. Biomed. Mater. 27 (2013) 154–166. [PubMed: 23491073]

[85]. Mohan D., Melvin JW, Failure properties of passive human aortic tissue. I - uniaxial tension tests, J. Biomech. 15 (1982) 887–902. [PubMed: 7161291]

[86]. Mohan D., Melvin JW, Failure properties of passive human aortic tissue. II - Biaxial tension tests, J. Biomech. 16 (1983) 31–44. [PubMed: 6833308]

[87]. Nakashima Y., Pathogenesis of aortic dissection: elastic fiber abnormalities and aortic medial weakness, Ann. Vasc. Dis. 3 (2010) 28–36. [PubMed: 23555385]

[88]. Nathan DP, Xu C., Gorman III JH, Fairman RM, Bavaria JE, Gorman RC, Chandran KB, Jackson BM, Pathogenesis of acute aortic dissection: a finite element stress analysis, Ann. Thorac. Surg. 91 (2011) 458–463. [PubMed: 21256291]

[89]. Niestrawska JA, Viertler C., Regitnig P., Cohnert TU, Sommer G., Holzapfel GA, Microstructure and mechanics of healthy and aneurysmatic abdominal aortas: experimental analysis and modeling, J.R. Soc. Interface 13 (2016) 20160620.

[90]. Noble C., Smulders N., Lewis R., Carré MJ, Franklin SE, MacNeil S., Taylor TA., Controlled peel testing ofa model tissue for diseased aorta, J. Biomech. 49 (2016) 3667–3675. [PubMed: 27743628]

[91]. Oberwalder PJ, Aneurysmen und Dissektionen der thorakalen Aorten: definition und Pathologie, J. Kardiol. 8 (2001) 2–4.

[92]. Okamoto RJ,Wagenseil JE, DeLong WR, Peterson SJ, Kouchoukos NT, Sundt TM, Mechanical properties of dilated human ascending aorta, Ann. Biomed. Eng. 30 (2002) 624–635. [PubMed: 12108837]

[93]. Olsson C., Thelin S., Stahle E., Ekbom A., Granath F., Thoracic aortic aneurysm and dissection: increasing prevalence and improved outcomes reported in a nationwide population-based study of more than 14,000 cases from 1987 to 2002, Circulation 114 (2006) 2611–2618. [PubMed: 17145990]

[94]. O'Connell MK, Murthy S., Phan S., Xu C., Buchanan J., Spilker R., Dalman RL, Zarins CK, Denk W., Taylor CA, The three-dimensional micro- and nanostructure of the aortic medial lamellar unit measured using 3D confocal and electron microscopy imaging, Matrix Biol. 27 (2008) 171–181. [PubMed: 18248974]

[95]. O'Leary SA, Mulvihill JJ, Barrett HE, Kavanagh EG, Walsh MT, McGloughlin T., Doyle BJ, Determining the influence of calcification on the failure properties of abdominal aortic aneurysm (AAA) tissue, J. Mech. Behav. Biomed. Mater. 42 (2015) 154–167. [PubMed: 25482218]

[96]. Pal S., Tsamis A., Pasta S., D'Amore A., Gleason TG, Vorp DA, Maiti S., A mechanistic model on the role of radially-running collagen fibers on dissection properties of human ascending thoracic aorta, J. Biomech. 47 (2014) 981–988. [PubMed: 24484644]

[97]. Pape LA, Awais M., Woznicki EM, Suzuki T., Trimarchi S., Evangelista A., Myrmel T., Larsen M., Harris KM, Greason K., Di Eusanio Bossone M., Montgomery DG, Eagle KA, Nienaber CA, Isselbacher EM, O'Gara P., Presentation, diagnosis, and outcomes of acute aortic dissection: 17-

year trends from the international registry of acute aortic dissection, J. Am. Coll. Cardiol. 66 (2015) 350–358. [PubMed: 26205591]

[98]. Pape LA, Tsai TT, Isselbacher EM, Oh JK, O'Gara PT, Evangelista A., Fattori R., Meinhardt G., Trimarchi S., Bossone E., Suzuki T., Cooper JV, Froehlich JB, Nienaber CA, Eagle KA, International Registry of Acute Aortic Dissection (IRAD) Investigators, Aortic diameter > or = 5.5 cm is not a good predictor of type A aortic dissection: Observations from the International Registry of Acute Aortic Dissection (IRAD), Circulation 116 (2007) 1120–1127. [PubMed: 17709637]

[99]. Pasta S., Phillippi JA, Gleason TG, Vorp DA, Effect of aneurysm on the mechanical dissection properties of the human ascending thoracic aorta, J. Thorac. Cardiovasc. Surg. 143 (2012) 460–467. [PubMed: 21868041]

[100]. Pearson R., Philips N., Hancock R., Hashim S., Field M., Richens D., McNally D., Regional wall mechanics and blunt traumatic aortic rupture at the isthmus, Eur. J. Cardiothorac. Surg. 34 (2008) 616–622. [PubMed: 18515136]

[101]. Peterss S., Mansour AM, Ross JA, Vaitkeviciute I., Charilaou P., Dumfarth J., Fang H., Ziganshin BA, Rizzo JA, Adeniran AJ, Elefteriades JA, Changing pathology of the thoracic aorta from acute to chronic dissection: literature review and insights, J. Am. Coll. Cardiol. 68 (2016) 1054–1065. [PubMed: 27585511]

[102]. Pham T., Martin C., Elefteriades J., Sun W., Biomechanical characterization of ascending aortic aneurysm with concomitant bicuspid aortic valve and bovine aortic arch, Acta Biomater. 9 (2013) 7927–7936. [PubMed: 23643809]

[103]. Phillippi JA, Green BR, Eskay MA, Kotlarczyk MP, Hill MR, Robertson AM, Watkins SC, Vorp DA, Gleason TG, Mechanism of aortic medial matrix remodeling is distinct in patients with bicuspid aortic valve, J. Thorac. Cardiovasc. Surg. 147 (2014) 1056–1064. [PubMed: 23764410]

[104]. Pichamuthu JE,Phillippi JA, Cleary DA, Chew DW,Hempel J., Vorp DA, Gleason TG, Differential tensile strength and collagen composition in ascending aortic aneurysms by aortic valve phenotype, Ann. Thorac. Surg. 96 (2013) 2147–2154. [PubMed: 24021768]

[105]. Polzer S., Gasser CT, Biomechanical rupture risk assessment of abdominal aortic aneurysms based on a novel probabilistic rupture risk index, J.R. Soc. Interface 12 (2015) 20150852.

[106]. Prijon T., Ermenc B., Classification of blunt aortic injuries a new systematic overview of aortic trauma, Forensic. Sci. Int. 195 (2010) 6–9. [PubMed: 19931340]

[107]. Purslow PP, Positional variations in fracture toughness, stiffness and strength of descending thoracic pig aorta, J. Biomech. 16 (1983) 947–953. [PubMed: 6654923]

[108]. Raghavan ML, Hanaoka MM, Kratzberg JA, de Lourdes Higuchi M., da Silva ES, Biomechanical failure properties and microstructural content of ruptured and unruptured abdominal aortic aneurysms, J. Biomech. 44 (2011)2501–2507. [PubMed: 21763659]

[109]. Raghavan ML, Kratzberg J., Castro de Tolosa EM, Hanaoka MM, Walker P., da Silva ES, Regional distribution of wall thickness and failure properties of human abdominal aortic aneurysm, J. Biomech. 39 (2006) 3010–3016. [PubMed: 16337949]

[110]. Raghavan ML, Webster MW, Vorp DA, Ex vivo biomechanical behavior of abdominal aortic aneurysm: assessment using a new mathematical model, Ann. Biomed. Eng. 24 (1996) 573–582. [PubMed: 8886238]

[111]. Rajagopal K., Bridges C., Rajagopal KR, Towards an understanding of the mechanics underlying aortic dissection, Biomech. Model. Mechanobiol. 6 (2007) 345–359. [PubMed: 17356838]

[112]. Reeps C., Maier A., Pelisek J., Hartl F., Grabher-Meier V., Wall WA, Essler M., Eckstein HH, Gee MW, Measuring and modeling patient-specific distributions of material properties in abdominal aortic aneurysm wall, Biomech. Model. Mechanobiol. 12 (2013) 717–733. [PubMed: 22955570]

[113]. Richens D., Field M., Neale M., Oakley C., Review: the mechanism of injury in blunt traumatic rupture of the aorta, Eur. J. Cardio-thorac. 21 (2002) 288–293.

[114]. Roach MR, Song SH, Variations in strength of the porcine aorta as a function of location, Clin. Invest. Med. 17 (1994) 308–318. [PubMed: 7982294]

[115]. Romo A., Badel P., Duprey A., Favre JP, Avril S., In vitro analysis of localized aneurysm rupture, J. Biomech. 47 (2014) 607–616. [PubMed: 24406100]

[116]. Ruddy JM, Jones JA, Ikonomidis JS, Pathophysiology of thoracic aortic aneurysm (TAA): is it not one uniform aorta? Role of embryologic origin, Prog. Cardiovasc. Dis. 56 (2013) 68–73. [PubMed: 23993239]

[117]. Saeyeldin AA, Velasquez CA, Mahmood SUB,Brownstein AJ, Zafar MA, Ziganshin BA,Elefteriades JA, Thoracic aortic aneurysm: unlocking the “silent killer” secrets, Gen. Thorac. Cardiovasc. Surg. 67 (2017) 1–11. [PubMed: 29204794]

[118]. Sassani SG, Tsangaris S., Sokolis DP, Layer- and region-specific material characterization of ascending thoracic aortic aneurysms by microstructure- based models, J. Biomech. 48 (2015) 3757–3765. [PubMed: 26476765]

[119]. Schermerhorn M., A 66-year-old man with an abdominal aortic aneurysm: review of screening and treatment, J. Am. Med. Assoc. 302 (2009) 2015–2022.

[120]. Schriefl AJ, Zeindlinger G., Pierce DM, Regitnig P., Holzapfel GA, Determination of the layer-specific distributed collagen fiber orientations in human thoracic and abdominal aortas and common iliac arteries, J.R. Soc. Interface 9 (2012) 1275–1286. [PubMed: 22171063]

[121]. Sevitt S., The mechanisms of traumatic rupture of the thoracic aorta, Br. J. Surg. 64 (1977) 166–173. [PubMed: 890257]

[122]. Shah SB, Witzenburg C., Hadi MF, Wagner HP, Goodrich JM, Alford PW, Barocas VH, Prefailure and failure mechanics of the porcine ascending thoracic aorta: experiments and a multiscale model, J. Biomech. Eng. 136 (2014). 021028–1.

[123]. Shahmansouri N., Alreshidan M., Emmott A., Lachapelle K., Cartier R., Leask RL, Mongrain R., Evaluating ascending aortic aneurysm tissue toughness: dependence on collagen and elastin contents, J. Mech. Behav. Biomed. Mater. 64 (2016) 262–271. [PubMed: 27526037]

[124]. Sherifova S., Sommer G., Viertler C., Regitnig P., Caranasos T., Smith MA, Griffith BE, Ogden RW, Holzapfel GA, Failure properties and microstructure of healthy and aneurysmatic human thoracic aortas with a focus on the media, Acta Biomater. (2019) submitted.

[125]. Shimizu K., Mitchell RN, Libby P., Inflammation and cellular immune responses in abdominal aortic aneurysms, Arterioscler. Thromb. Vasc. Biol. 26 (2006) 987–994. [PubMed: 16497993]

[126]. Shkrum MJ, McClafferty KJ, Green RN, Nowak ES,Young JG, Mechanisms of aortic injury in fatalities occurring in motor vehicle collisions, J. Forensic Sci. 44 (1999) 44–56. [PubMed: 9987869]

[127]. Sokolis DP, Iliopoulos DC, Impaired mechanics and matrix metalloproteinases/inhibitors expression in female ascending thoracic aortic aneurysms, J. Mech. Behav. Biomed. Mater. 34 (2014) 154–164. [PubMed: 24583920]

[128]. Sokolis DP, Kritharis EP, Giagini AT, Lampropoulos KM, Papadodima SA, Iliopoulos DC, Biomechanical response of ascending thoracic aortic aneurysms: association with structural remodelling, Comput. Methods Biomech. Biomed. Eng. 15 (2012) 231–248.

[129]. Sokolis DP, Kritharis EP, Iliopoulos DC, Effect oflayer heterogeneity on the biomechanical properties of ascending thoracic aortic aneurysms, Med. Biol. Eng. Comput. 50 (2012) 1227–1237. [PubMed: 22926448]

[130]. Sommer G., Gasser TC, Regitnig P., Auer M., Holzapfel GA, Dissection properties of the human aortic media: an experimental study, J. Biomech. Eng. 130 (2008). 021007–1-12.

[131]. Sommer G., Sherifova S., Oberwalder PJ, Dapunt OE, Ursomanno PA, DeAnda A., Griffith BE, Holzapfel GA, Mechanical strength of aneurysmatic and dissected human thoracic aortas at different shear loading modes, J. Biomech. 49 (2016) 2374–2382. [PubMed: 26970889]

[132]. Soyer R., Bessou JP, Bouchart F., Tabley A., Mouton-Schleifer D., Arrignon J., Redonnet M., Acute traumatic isthmic aortic rupture: Long-term results in 49 patients, Eur. J. Cardiothorac. Surg. 6 (1992) 431–437. [PubMed: 1389250]

[133]. Stary HC, Atlas of Atherosclerosis: Progression and Regression, second ed, The Parthenon Publishing Group, Boca Raton, London, New York, Washington, D.C., 2003.

[134]. Sugita S., Matsumoto T., Heterogeneity of deformation of aortic wall at the microscopic level: contribution of heterogeneous distribution of collagen fibers in the wall, Biomed. Mater. Eng. 23 (2013) 447–461. [PubMed: 24165548]

[135]. Sugita S., Matsumoto T., Novel biaxial tensile test for studying aortic failure phenomena at a microscopic level, Biomed. Eng. Online 12 (2013) 3. [PubMed: 23305508]

[136]. Sugita S., Matsumoto T., Local distribution of collagen fibers determines crack initiation site and its propagation direction during aortic rupture, Biomech. Model. Mechanobiol. 17 (2018) 577–587. [PubMed: 29134291]

[137]. Sugita S., Matsumoto T., Ohashi T., Kumagai K., Akimoto H., Tabayashi K., Sato M., Evaluation of rupture properties of thoracic aortic aneurysms in a pressure-imposed test for rupture risk estimation, Cardiovasc. Eng. Technol. 3 (2012) 41–51.

[138]. Svensson LG, Kouchoukos NT, Miller DC, Bavaria JE, Coselli JS, Curi MA, Eggebrecht H., Elefteriades JA, Erbel R., Gleason TG, Lytle BW, Mitchell RS, Nienaber CA, Roselli EE, Safi HJ, Shemin RJ, Sicard GA, Sundt TM 3rd, Szeto WY, Wheatley GH 3rd, Society of Thoracic Surgeons Endovascular Surgery Task Force, Expert consensus document on the treatment of descending thoracic aortic disease using endovascular stent-grafts, Ann. Thorac. Surg. 85 (2008) S1–S41. [PubMed: 18083364]

[139]. Tam ASM, Sapp MC, Roach MR, The effect of tear depth on the propagation of aortic dissections in isolated porcine thoracic aorta, J. Biomech. 31 (1998) 673–676. [PubMed: 9796691]

[140]. Thubrikar MJ, Labrosse M., Robicsek F., Al-Soudi J., Fowler B., Mechanical properties of abdominal aortic aneurysm wall,J. Med. Eng. Technol. 25 (2001) 133–142. [PubMed: 11601439]

[141]. Tiessen IM, Roach MR, Factors in the initiation and propagation of aortic dissections in human autopsy aortas, J. Biomech. Eng. 115 (1993) 123–125. [PubMed: 8445891]

[142]. Tong J., Cheng Y., Holzapfel GA, Mechanical assessment of arterial dissection in health and disease: advancements and challenges, J. Biomech. 49 (2016) 2366–2373. [PubMed: 26948576]

[143]. Tong J., Cohnert T., Regitnig P., Kohlbacher J., Birner-Gruenberger R., Schriefl AJ, Sommer G., Holzapfel GA, Variations of dissection properties and mass fractions with thrombus age in human abdominal aortic aneurysms, J. Biomech. 47 (2014) 14–23. [PubMed: 24309621]

[144]. Trabelsi O., Davis FM, Rodriguez-Matas JF, Duprey A., Avril S., Patient specific stress and rupture analysis of ascending thoracic aneurysms, J. Biomech. 48 (2015) 1836–1843. [PubMed: 25979384]

[145]. Trabelsi O., Gutierrez M., Farzaneh S., Duprey A., Avril S., A non-invasive methodology for ATAA rupture risk estimation, J. Biomech. 66 (2018) 119–126. [PubMed: 29180233]

[146]. Tsamis A., Phillippi JA, Koch RG, Chan PG, Krawiec JT, D'Amore A., Watkins SC, Wagner WR, Vorp DA, Gleason TG, Extracellular matrix fiber microarchitecture is region-specific in bicuspid aortic valve-associated ascending aortopathy, J. Thorac. Cardiovasc. Surg. 151 (2016) 1718–1728.e5. [PubMed: 26979916]

[147]. Tsamis A., Phillippi JA, Koch RG, Pasta S., D'Amore A., Watkins SC, Wagner WR, Gleason TG, Vorp DA, Fiber micro-architecture in the longitudinal-radial and circumferential-radial planes of ascending thoracic aortic aneurysm media, J. Biomech. 46 (2013) 2787–2794. [PubMed: 24075403]

[148]. Uzel SGM, Buehler MJ, Molecular structure, mechanical behavior and failure mechanism of the C-terminal cross-link domain in type I collagen, J. Mech. Behav. Biomed. Mater. 4 (2011) 153–161. [PubMed: 21262493]

[149]. Vallabhaneni SR, Gilling-Smith GL, How TV, Carter SD, Brennan JA, Harris PL, Heterogeneity of tensile strength and matrix metalloproteinase activity in the wall of abdominal aortic aneurysms, J. Endovasc. Ther. 11 (2004) 494–502. [PubMed: 15298501]

[150]. Vande Geest JP, Dillavou ED, Di Martino ES, Oberdier M., Bohra A., Makaroun MS, Vorp DA, Gender-related differences in the tensile strength of abdominal aortic aneurysm, Ann. N.Y. Acad. Sci. 1085 (2006) 400–402. [PubMed: 17182963]

[151]. Vande Geest JP, Di Martino ES, Bohra A., Makaroun MS, Vorp DA, A biomechanics-based rupture potential index for abdominal aortic aneurysm risk assessment: demonstrative application, Ann. N.Y. Acad. Sci. 1085 (2006) 11–21. [PubMed: 17182918]

[152]. Vande Geest JP, Wang DHJ, Wisniewski SR, Makaroun MS, Vorp DA, Towards a noninvasive method for determination of patient-specific wall strength distribution in abdominal aortic aneurysms, Ann. Biomed. Eng. 34 (2006) 1098–1106. [PubMed: 16786395]

[153]. Viano D., Biomechanics of nonpenetrating aortic trauma: a review, SAE Technical Paper 831608 (1983) 109–114.

[154]. Vorp DA, Biomechanics of abdominal aortic aneurysm,J. Biomech. 40 (2007) 1887–1902. [PubMed: 17254589]

[155]. Vorp DA, Lee PC, Wang DH, Makaroun MS, Nemoto EM, Ogawa S., Webster MW, Association of intraluminal thrombus in abdominal aortic aneurysm with local hypoxia and wall weakening, J. Vasc. Surg. 34 (2001) 291–299. [PubMed: 11496282]

[156]. Vorp DA, Raghavan ML, Muluk SC, Makaroun MS, Steed DL, Shapiro R., Webster MW, Wall strength and stiffness of aneurysmal and nonaneurysmal abdominal aorta, Ann. N.Y Acad. Sci. 800 (1996) 274–276. [PubMed: 8959012]

[157]. Vorp DA, Schiro BJ, Ehrlich MP, Juvonen TS, Ergin MA, Griffith BP, Effect of aneurysm on the tensile strength and biomechanical behavior of the ascending thoracic aorta, Ann. Thorac. Surg. 800 (2003) 1210–1214.

[158]. Wang L., Zhang J., Fu W., Guo D., Jiang J., Wang Y., Association of smooth muscle cell phenotypes with extracellular matrix disorders in thoracic aortic dissection, J. Vasc. Surg. 56 (2012) 1698–1709. [PubMed: 22960022]

[159]. Wang X., LeMaire SA, Chen L., Shen YH, Gan Y., Bartsch H., Carter SA, Utama B., Ou H., Coselli JS, Wang XL, Increased collagen deposition and elevated expression of connective tissue growth factor in human thoracic aortic dissection, Circulation 114 (2006). I–200–I–205.

[160]. Whelan A., Duffy J., Gaul RT, O'Reilly D., Nolan DR, Gunning P., Lally C., Murphy BP, Collagen fibre orientation and dispersion govern ultimate tensile strength, stiffness and the fatigue performance of bovine pericardium, J. Mech. Behav. Biomed. Mater. 90 (2019) 54–60. [PubMed: 30343171]

[161]. Wilson H., Roome NW, Traumatic shock syndrome following rupture of the aorta and multiple fractures, Am. J. Surg. 23 (1933) 333.

[162]. Wittek A., Hawkins T., Miller K., On the unimportance of constitutive models in computing brain deformation for image-guided surgery, Biomech. Model. Mechanobiol. 8 (2009) 77–84. [PubMed: 18246376]

[163]. Witzenburg CM, Dhume RY, Shah SB, Korenczuk CE, Wagner HP, Alford PW, Barocas VH, Failure of the porcine ascending aorta: multidirectional experiments and a unifying microstructural model, J. Biomech. Eng. 139 (2017). 031005–031005-14.

[164]. Wolinsky H., Comparison of medial growth ofhuman thoracic and abdominal aortas, Circ. Res. 27 (1970) 531–538. [PubMed: 5507030]

[165]. Wolinsky H., Glagov S., A lamellar unit of aortic medial structure and function in mammals, Circ. Res. 20 (1967) 90–111.

[166]. Wolinsky H., Glagov S., Comparison of abdominal and thoracic aortic medial structure in mammals. deviation of man from the usual pattern, Circ. Res. 25 (1969) 677–686. [PubMed: 5364644]

[167]. Wu D., Shen YH, Russell L., Coselli JS, LeMaire SA, Molecular mechanisms of thoracic aortic dissection, J. Surg. Res. 184 (2013) 907–924. [PubMed: 23856125]

[168]. Zehnder MA, Delayed post-traumatic rupture of the aorta in a young healthy individual after closed injury; mechanical-etiological considerations, Angiology 7 (1956) 252–267. [PubMed: 13327310]

[169]. Zitnay JL, Li Y., Qin Z., San BH, Depalle B., Reese SP, Buehler MJ, Yu SM, Weiss JA, Molecular level detection and localization of mechanical damage in collagen enabled by collagen hybridizing peptides, Nat. Commun. 8 (2017) 14913. [PubMed: 28327610]

Statement of Significance

Aortic dissections and aortic aneurysms are fatal events characterized by structural changes to the aortic wall. Despite the advances in medical, biomedical and biomechanical research, the mortality rates of aneurysms and dissections remain high. The present review article summarizes experimental studies that quantify the aortic wall strength and it discusses biomechanically motivated models to predict rupture risk. We identified contradictory observations and a large variation within and between data sets, which may be due to biological variations, different sample sizes, differences in experimental protocols, etc. Based on the findings of the reviewed literature and the rather large variations in tissue strength, it is proposed that an appropriate criterion for aortic failure should also reflect the microstructure.

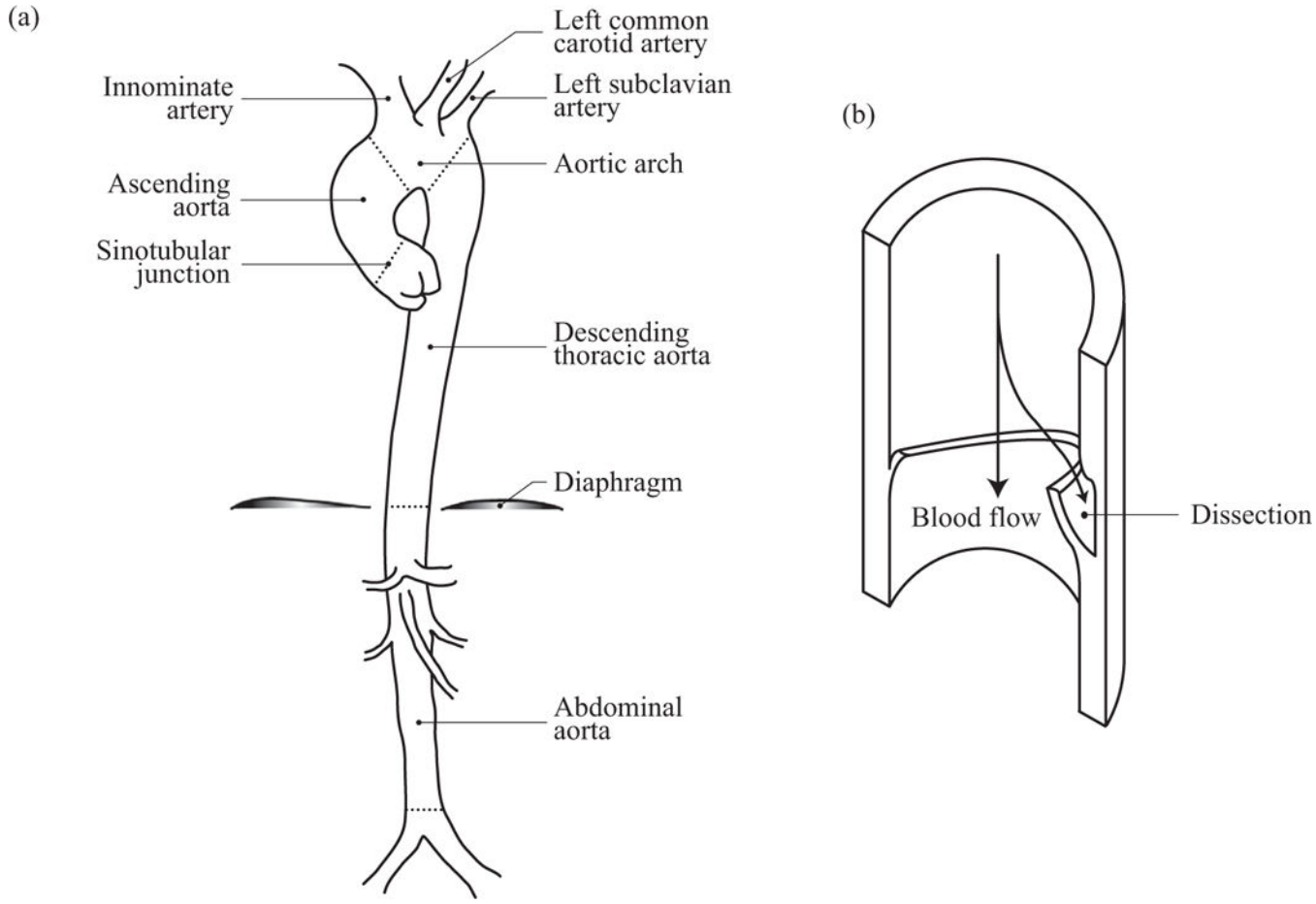

Fig. 1.

(a) Anatomy of the aorta with some of its branches; (b) sketch of a dissected wall with arrows indicating the blood flow.

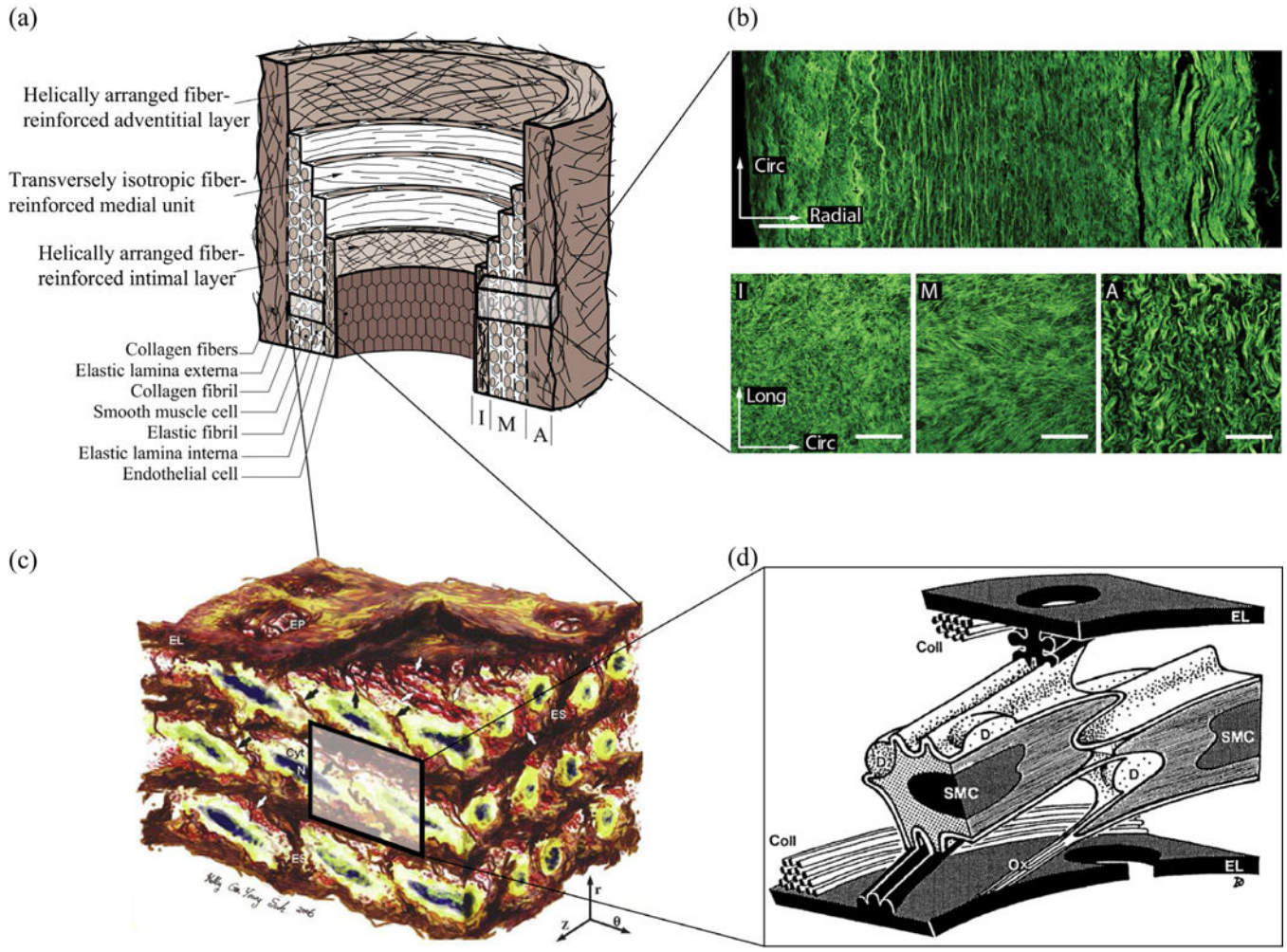

Fig. 2.

Structure of the aorta: (a) healthy but aged aortic wall with non-atherosclerotic intimal thickening composed of three layers – intima (I), media (M) and adventitia (A). Republished with permission from Gasser et al. [40]; (b) layered collagen architecture of a healthy and aged abdominal aorta – more specifically the top image depicts the out-of-plane structure in the circumferential-radial plane, while the three images at the bottom show in-plane sections of the intima (I), media (M) and adventitia (A) (white scale bars corresponding to 100 μm. Republished with permission from Niestrawska et al. [89]; (c) 3D microstructure of an aortic media consisting of several lamellar units –circumferentially-oriented radially-tilted smooth muscle cells (SMCs) with elliptical nuclei (N) sandwiched between elastic lamellas (EL) surrounded by a dense network of interlamellar elastin fibers (IEFs shown with black arrows), elastin struts (ES), and reinforced elastin pores (EP). Reprinted from O'Connell et al. [94], with permission from Elsevier; (d) schematic representation of two SMCs and two fenestrated EL with their interconnections – more specifically, collagen fibers (Coll) are closely associated with EL, surface ridges of the left SMC are connected to both EL via elastin protrusions, right SMC is connected to the lower El via oxytalan fiber (Ox), and larger deposits (D) containing collagen and heparan sulfate proteoglycan are found at

indentations of the cell surface. Reprinted from Dingemans et al. [29], with permission from John Wiley and Sons.

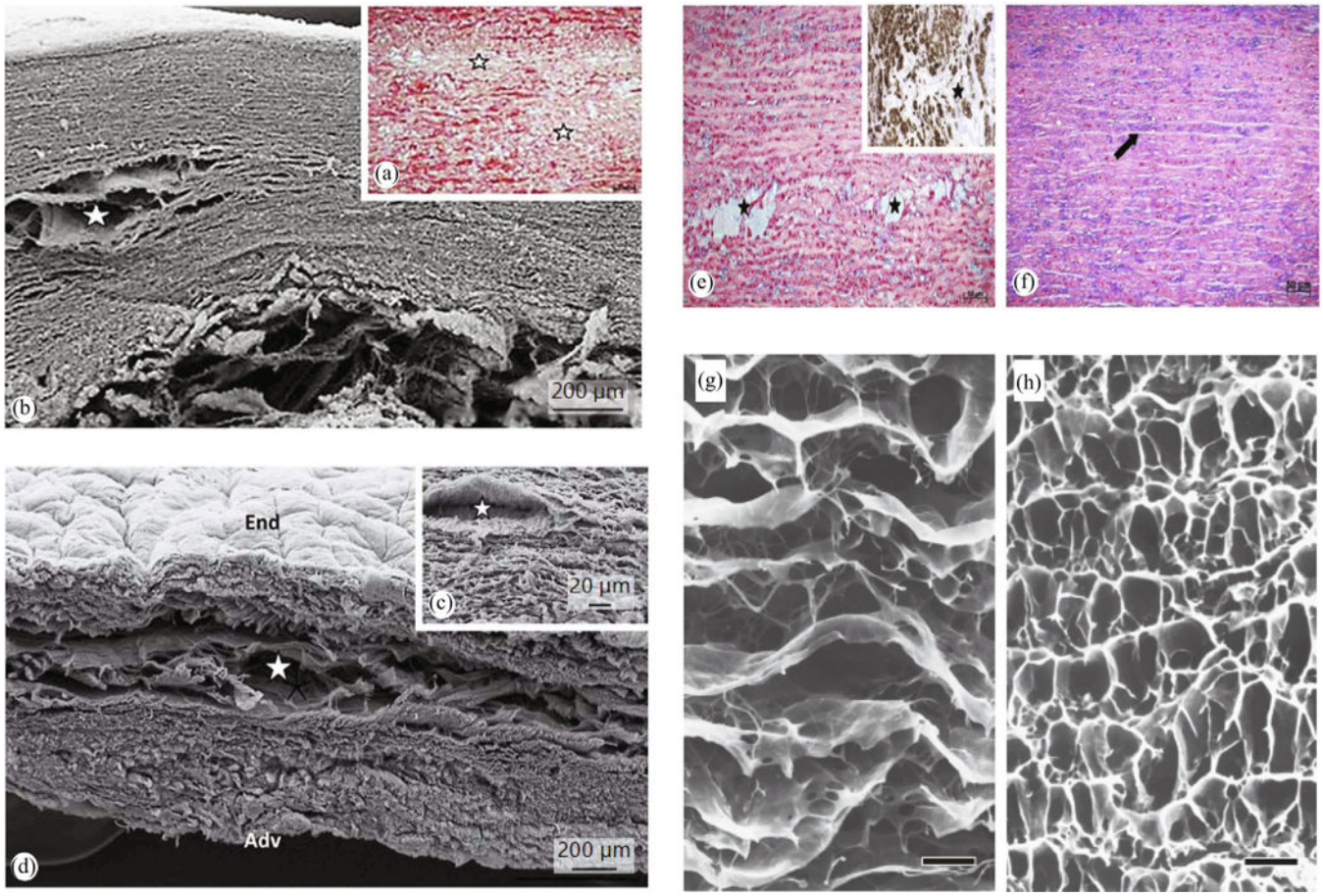

Fig. 3.

Microstructural changes due to pathological formations in human thoracic aortas with stars indicating mucoid accumulation areas (proteoglycan pools): (a), (b) disorganized collagen network visualized by (a) a histological section stained by picrosirius - collagen framework is disorganized - and (b) scanning electron microscopy (SEM); (c), (d) SEM images showing a lamellar structure disrupted probably by the proteoglycan pools (star) (Adv = Adventitia; End = endothelium coverage of the luminal face). Reprinted from Borges et al. [6] (Copyright © 2013 Karger Publishers, Basel, Switzerland); (e), (f) histological sections stained byAlcian blue showing (e) a pathological aorta with areas of mucoid accumulations (stars) - inset shows immunostaining for α-actin demonstrating the absence of SMCs inside the mucoid area; (f) control aorta where the space between elastic lamellae (arrow) is occupied by SMCs, collagen, and a normal amount of mucoid substance (light blue). Reprinted from Borges et al. [8], with permission from Elsevier; (g), (h) SEM images depicting the elastic fiber architecture of human aortic medias from (g) an aortic dissection patient and (h) a control subject (black scale bars indicate 20 μm. Reprinted from Nakashima [87] (licensed under CC BY-NC-SA 2.1 JP).

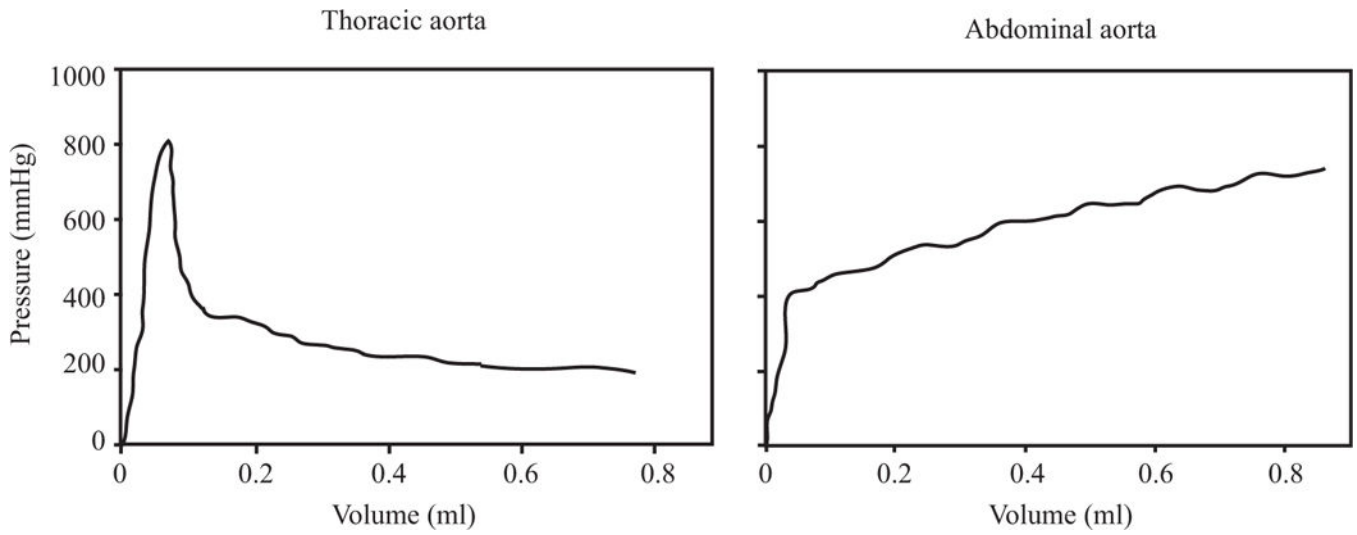

Fig. 4.

Pressure volume curves to create a bleb in the thoracic and abdominal sections of the aorta. Reprinted from Roach & Song [114], with permission from Clin. Invest. Med.

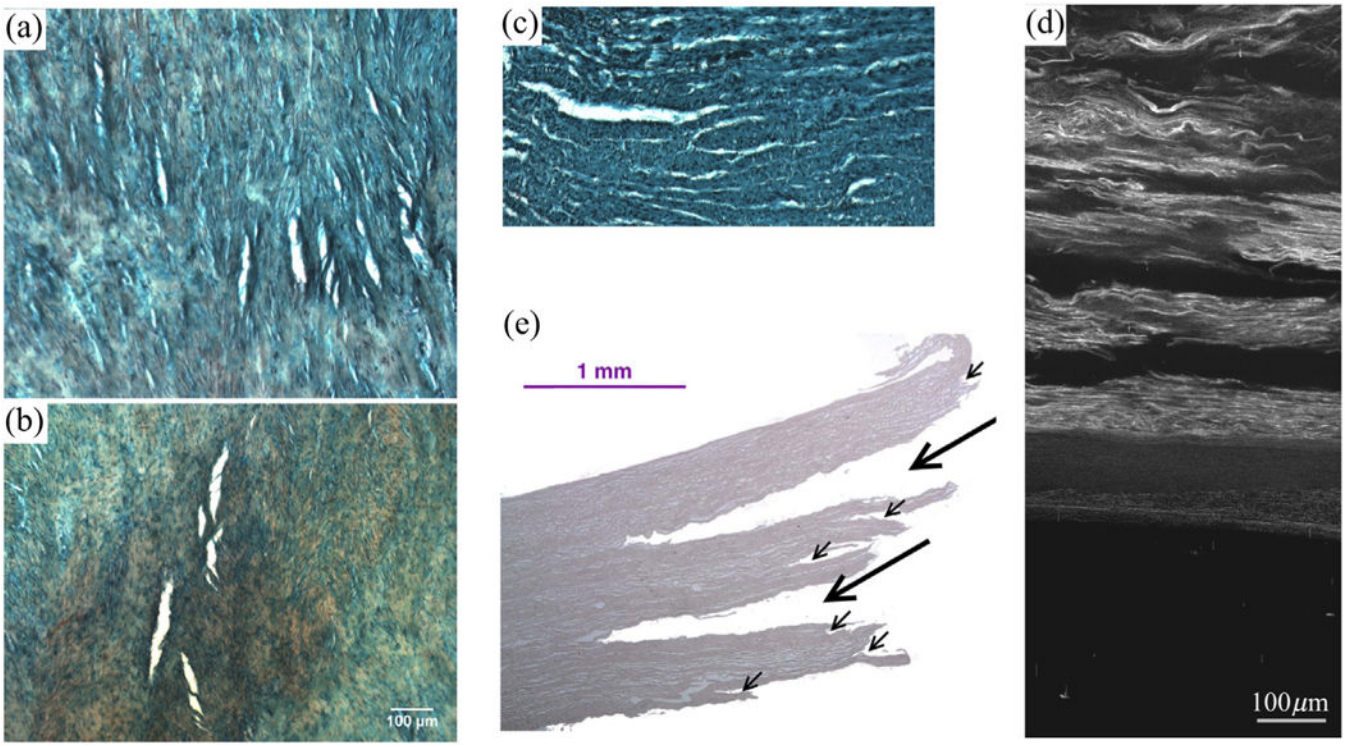

Fig. 5.

Initiation/propagation of aortic dissections due to shear stresses: (a)-(c) cracks visible after a block shear test, where the white areas are openings in the tissue. Reprinted from Haslach, Jr. et al. [47] with permission from Springer Nature; (a), (b) are slices in the circumferential-longitudinal plane where the horizontal direction is longitudinal - (a) circumferential deformation parallel to the collagen fibers and (b) longitudinal deformation; (c) slice in the radial-circumferential plane after circumferential deformation, where the horizontal direction is circumferential; (d) cracks visible as black zones between the lamellae in the radial-circumferential plane after an in-plane shear test in the circumferential direction. Reprinted from Sommer et al. [131], with permission from Elsevier; (e) cracks that occurred during a uniaxial test indicated by black arrows. Reprinted from Helfenstein-Didier et al. [50], with permission from Elsevier.

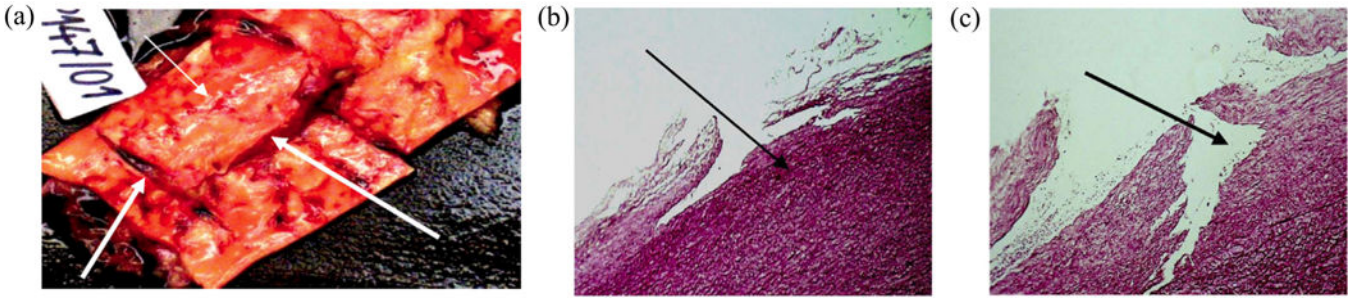

Fig. 6.

Aortic dissection and rupture due to traumatic injury. Reprinted from Prijon & Ermenc [106], with permission from Elsevier: (a) case presenting multiple ruptures: intramural and transmural, latter both in circumferential and longitudinal directions indicated by white arrows; (b) intramural rupture of the intima; (c) intramural rupture of the intima and the media.

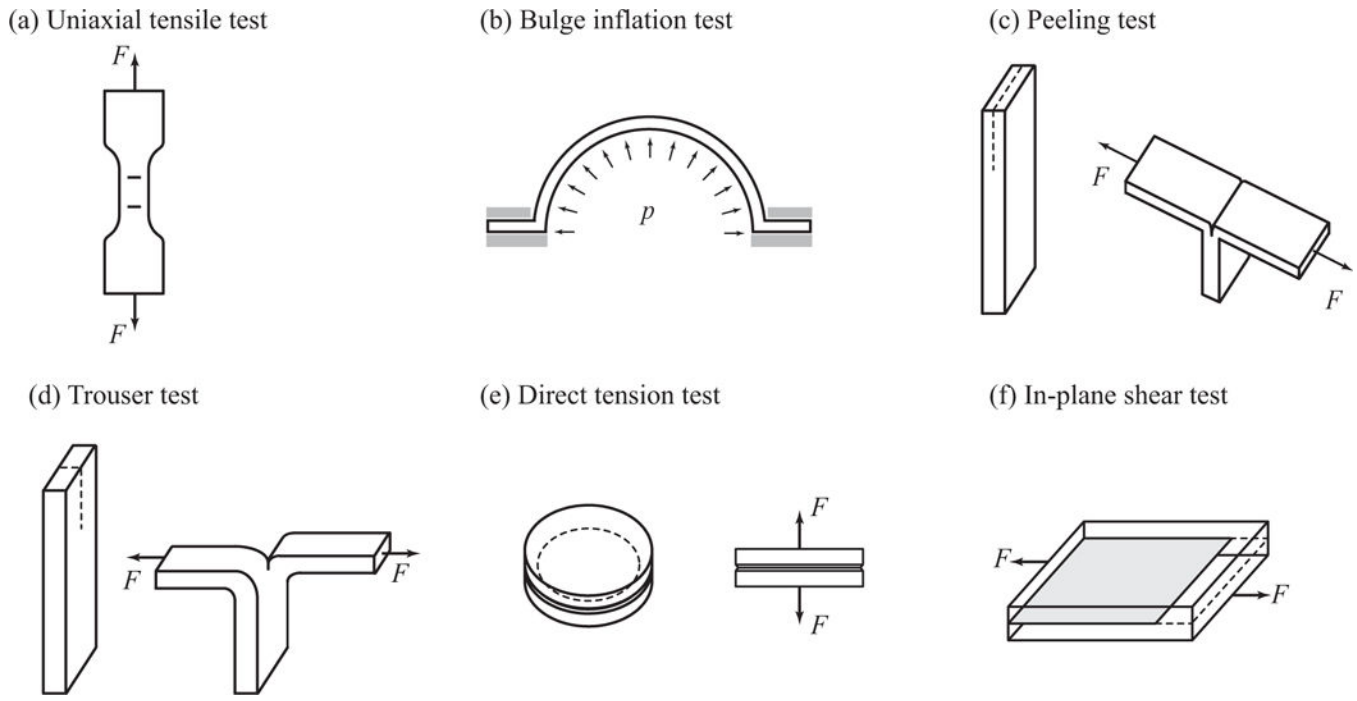

Fig. 7.

Experimental tests typically used to quantify the failure properties of aortas: (a) bone-shaped specimen for a uniaxial tensile test with load F; (b) bulge inflation test with pressure load p; (c) peeling test; (d) trouser test, as used in, e.g., Purslow [107]; (e) direct tension test to quantify radial strength, as used in, e.g., Sommer et al. [130,131]; (f) in-plane shear test with the sheared plane indicated in gray, as used in, e.g., Sommer et al. [131]. Black arrows and dashed lines indicate the load direction and the incision, respectively. Tests (a), (c), (d) and (f) can be performed in any tissue direction in the tangential plane.

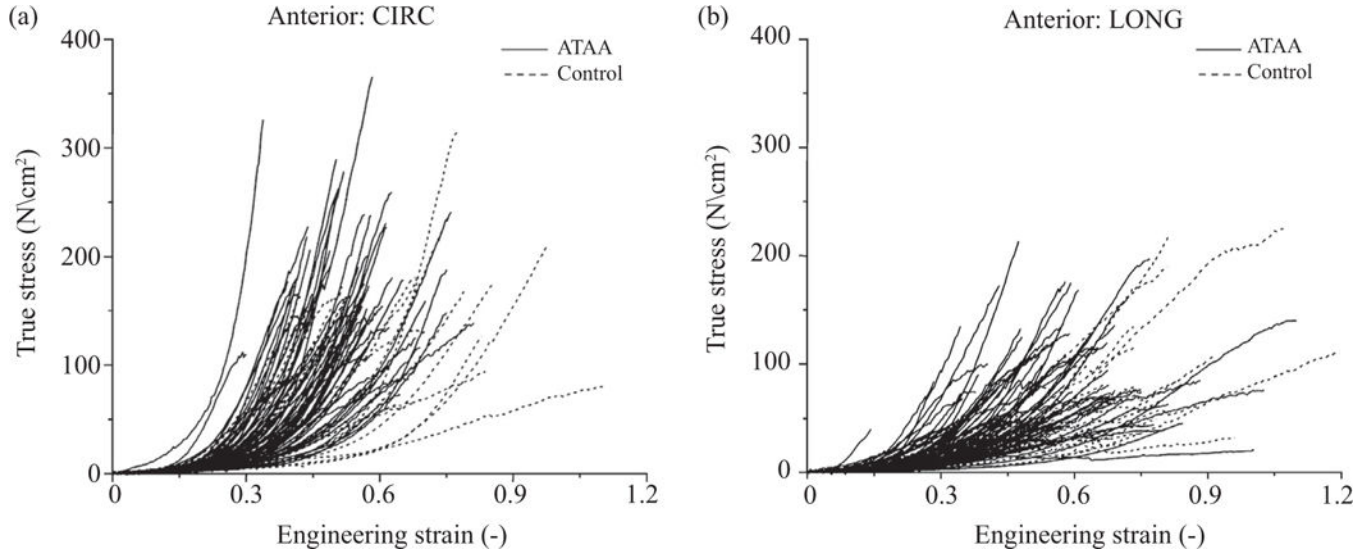

Fig. 8.

Stress-strain data of ascending thoracic aortic aneurysm (ATAA) and control specimens taken from the anterior region with (a) circumferential and (b) longitudinal orientation obtained from uniaxial tensile tests. Data show a large variability in failure properties. Reprinted from Iliopoulos et al. [56], with permission from Elsevier.

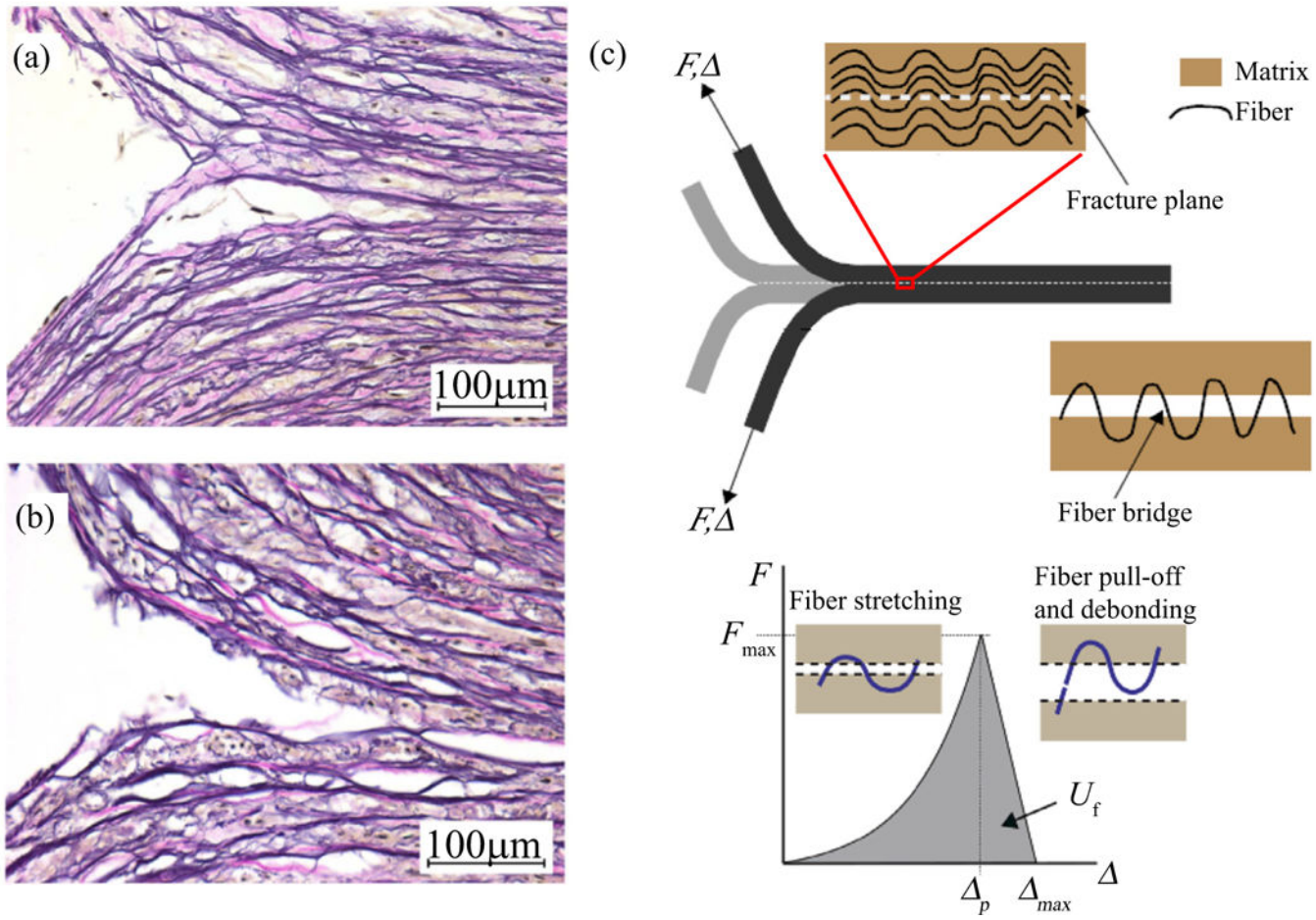

Fig. 9.

Histological images (Elastica van Gieson) of the dissection tips obtained from a peeling test of an aortic media during peeling in (a) circumferential and (b) longitudinal directions. Republished from Sommer et al. [130], Copyright © 2008 ASME, permission conveyed through CCC, Inc. The images highlight the irreversible mechanism of the separation at the microscopic level. (c) Schematic of fiber bridging failure; the matrix is already separated but still connected by an unruptured fiber (above); force-separation law (F vs Δ) for a collagen fiber bridge with nonlinear loading and linear post peak behavior starting at F_{max} and related Δ_p (below) - modes of fiber deformation and failure are depicted in the insets. Shaded region represents the energy U_f required for failure of the fiber bridge. Reprinted from Pal et al. [96], with permission from Elsevier.

Table 1

Overview of uniaxial tensile test results on aortas - tests performed until failure: ABA, abdominal aorta; AN, aneurysmatic; ASA, ascending aorta; BAV, bicuspid aortic valve; Circ, circumferential; DTA, descending thoracic aorta; H, healthy; Long, longitudinal; TAV, tricuspid aortic valve;

Study	Species	Location	Healthy/ Diseased	Additional information	Direction	*n*	Failure stress (kPa)	Failure stretch (−)
Mohan & Melvin [85]	Human	DTA	H	Quasi-static	Circ	18	1720±890	1.23 ± 0.28
					Long	18	1470±910	1.47 ± 0.23
				Dynamic	Circ	$16^{+},17^{*}$	5070±3290	1.60 ± 0.28
					Long	$18^{+},21^{*}$	3590 ±2040	1.64 ± 0.28
Raghavan et al. [110]	Human	ABA	H	–	Long	7	2014±394	–
			AN	–	Circ	16	1019±160	–
					Long	45	864±102	–
Vorp et al. [155]	Human	ABA	AN	ILT > 4 mm	Circ	7	1380±190	–
				ILT < 4 mm	Circ	7	2160±340	–
Vorp et al. [157]	Human	ASA	H	–	Circ	7	1800±240	–
					Long	7	1710±140	–
			AN	–	Circ	23	1180±120	–
					Long	17	1210±90	–
Di Martino et al. [28]	Human	ABA	AN	Ruptured	Circ	13	540 ± 60	–
				Unruptured	Circ	26	820 ± 90	–
Vande Geest et al. [152]	Human	ABA	AN	For model input	Circ	60	805 ± 60	–
				For validation	Circ	21	832 ± 85	–
García-Herrera et al. [39]	Human	ASA	H	< 35 yrs	Circ	–	2180±240	2.35 ± 0.1
					Long	–	1140±100	2.00 ± 0.1
				> 35 yrs	Circ	–	1200±200	–
					Long	–	660 ± 70	–
			AN	BAV	Circ	–	1230±150	1.80 ± 0.08
					Long	–	840±100	1.58 ± 0.06
				TAV	Circ	–	1190±130	–
					Long	–	880±120	–
Pichamuthu et al. [104]	Human	ASA	AN	BAV	Circ	–	1656±98	1.92 ± 0.04

Study	Species	Location	Healthy/ Diseased	Additional information	Direction	*n*	Failure stress (kPa)	Failure stretch (–)
					Long	–	698 ± 31	1.63 ± 0.02
				TAV	Circ	–	961 ± 61	1.61 ± 0.04
					Long	–	540 ± 37	1.47 ± 0.03
Shah et al. [122]	Porcine	ASA	–	–	Circ	11	2510 ± 439.3	1.99 ± 0.07
					Long	11	750 ± 102.6	1.92 ± 0.16
Ferrara et al. [35]	Human	ASA	AN	Anterior	Circ	37	1440 ±700	1.35 ± 0.16
					Long	34	940 ±490	1.34 ± 0.15
				Posterior	Circ	32	1850±700	1.36 ± 0.12
					Long	19	740±180	1.31 ± 0.09
Sommer et al. [131]	Human	ASA	AN	Media	Circ	7	1282 ±822	1.52 ± 0.20
					Long	10	565 ±198	1.52 ± 0.18

≠ values for stress;

* values for extension.

Table 2

Overview of bulge inflation test results on aortas: AN, aneurysmatic; ASA, ascending aorta; Circ, circumferential; DTA, descending thoracic aorta; Long, longitudinal; TA, thoracic aorta;

Study	Species	Location	Healthy/ Diseased	Speed (mm/min)	Additional information	Direction	*n*	Failure stress (kPa)	Failure extension (−)
Marra et al. [76]	Porcine	TA	–	60	–	Long	25	1750±710	1.523 ± 0.178[c]
Pearson et al. [100]	Porcine	ASA	–	–	–	–	10	3699 ±789	1.85 ± 0.114[d]
		DTA	–			–	10	4260±1626	1.70 ± 0.138[d]
		Isthmus	–			–	10	3248 ±1430	1.66 ± 0.109[d]
Kim et al. [64]	Human	ASA	AN	15	Media	Circ	6	547.5 ± 362.6	0.192 ± 0.08[e]
						Long	6	335.3 ± 103.8	0.261 ± 0.117[e]
					Adventitia	Circ	3	636.6 ± 322.7	0.252 ± 0.091[e]
						Long	3	976 ± 247.2	0.343 ± 0.123[e]
Sugita et al. [137]	Porcine	TA	–	15	Proximal	–	6	1810±430[a]	–
					Distal	–	6	2290 ±740[a]	–
	Human	TA	AN		–	–	6	980±390[a]	–
Romo et al. [115]	Human	ASA	AN	15	Media	–	9	780 ± 200[b]	–
					Adventitia	–	6	1460±103[b]	–
Duprey et al. [32]	Human	ASA	AN	15	Composite	–	31	1260±940[b]	1.37 ± 0.15[f]

[a] Laplace stress;

[b] stress perpendicular to the crack direction;

[c] mean stretch;

[d] circumferential stretch;

[e] average Green-Lagrange strain;

[f] stretch perpendicular to the crack direction.

Table 3

Overview of peeling test results on aortas: A, adventitia; ABA, abdominal aorta; Age*, age of intraluminal thrombus; AM, adventitia + media; AN, aneurysmatic; AT, atherosclerosis; ASA, ascending aorta; BAV, bicuspid aortic valve; Circ, circumferential; *F*/*w*, force per width; Long, longitudinal; H, healthy; MI, media + intima; TA, thoracic aorta; TAV, tricuspid aortic valve; W_{diss}, dissection energy; $^{+}$ according to [133].

Study	Species	Location	Healthy/ Diseased	Additional information	Direction	*n*	*F*/*w* (mN/mm)	W_{diss} (mJ/cm^2)
Sommer et al. [130]	Human	ABA	H	Media	Circ	5	22.9 ± 2.9	5.1 ± 0.6
					Long	7	34.8 ± 15.5	7.6 ± 2.7
Pasta et al. [99]	Human	ASA	H	Control	Circ	7	126 ± 6.6	–
					Long	7	149 ± 7.6	–
			AN	TAV	Circ	8	109.1 ± 5.2	–
					Long	8	116.8 ± 6.1	–
				BAV	Circ	16	88.4 ± 4.1	–
					Long	16	100 ± 4.1	–
Tong et al. [143]	Human	ABA	AN	Age* II, A	Circ	11	–	10.1 ± 1.7
					Long	9	–	9.3 ± 0.9
				Age* III, A	Circ	8	–	9.2 ± 2.0
					Long	7	–	8.3 ± 1.3
				Age* IV, A	Circ	6	–	8.6 ± 1.4
					Long	7	–	7.8 ± 1.0
				Age* II, MI	Circ	12	–	6.7 ± 1.2
					Long	12	–	8.4 ± 1.9
				Age* III, MI	Circ	8	–	5.5 ± 1.1
					Long	8	–	6.8 ± 1.7
				Age* IV, MI	Circ	7	–	4.2 ± 1.1
					Long	6	–	5.1 ± 1.4
Kozuń [66]	Human	TA	AT	A-MI	Circ	26	24.5 ± 7.5	5.6 ± 0.9
			(stage II^{+})		Long	7	32.4 ± 6.5	7.6 ± 1.7
				AM-I	Circ	22	26.5 ± 6.7	4.1 ± 1.0
					Long	8	34.2 ± 3.5	4.7 ± 0.9
Noble et al. [90]	Porcine	TA	–	Control	Circ	16	67.4 ± 11.7	15.18 ± 2.70

Study	Species	Location	Healthy/ Diseased	Additional information	Direction	*n*	*F/w* (mN/mm)	W_{diss} (mJ/cm^2)
					Long	16	76.7 ± 25.9	18.33 ± 6.42
				Collagenase	Circ	17	49.3 ± 11.9	10.81 ± 2.80
					Long	14	53.9 ± 12.2	13.58 ± 3.12
				Elastase	Circ	16	58.8 ± 17.3	13.24 ± 4.00
					Long	14	69.1 ± 27.0	17.18 ± 7.12
				Glutaraldehyde treatment	Circ	13	91.2 ± 28.2	19.01 ± 6.05
					Long	14	83.6 ± 13.7	18.63 ± 3.35